2018

Novel Technique of Fabrication of Porous Copper and Copper Oxide to Improve the Lithium Ion Battery Performance

Raju Prasad Ghimire
South Dakota State University

NOVEL TECHNIQUE OF FABRICATION OF POROUS COPPER AND COPPER OXIDE TO IMPROVE THE LITHIUM ION BATTERY PERFORMANCE

BY

RAJU PRASAD GHIMIRE

A thesis submitted in partial fulfillment of the requirements for the

Master of Science

Major in Electrical Engineering

South Dakota State University

2018

NOVEL TECHNIQUE OF FABRICATION OF POROUS COPPER AND COPPER OXIDE TO IMPROVE THE LITHIUM ION BATTERY PERFORMANCE

RAJU PRASAD GHIMIRE

This thesis is approved as a creditable and independent investigation by a candidate for the Master of Science degree in Electrical Engineering and is acceptable for meeting the thesis requirements for this degree. Acceptance of this thesis does not imply that the conclusions reached by the candidate are necessarily the conclusions of the major department.

Qiquan Qiao, Ph.D. Date
Thesis Advisor

George Hamer, Ph.D. Date
Head, Department of Electrical
Engineering and Computer Science

Dean, Graduate School Date

I would like to dedicate my thesis to my beloved wife (Bhawana Paudel), daughter (Zoya Ghimire), maternal-uncle (Doleswar Bhandari), maternal-aunt (Manju Bhandari Ghimire), brothers (Durga Prasad Ghimire and Santosh Ghimire) and my beloved parents, Nagendra Prasad Ghimire and Gita Devi Ghimire for their love, support and encouragement. Without their support, I would not be able to make this happen.

ACKNOWLEDGEMENTS

The work presented in this thesis was supported by NASA EPSCoR (Award #: NNX14AN22A), NSF MRI program, and department of physics of South Dakota State University.

First and foremost, I would extend my deepest gratitude to Dr. Qiquan Qiao, my supervisor and graduate coordinator, for providing me the opportunity of working in his research group as a research assistant and his enormous help throughout this project.

Humbly, my appreciation goes to Dr. Parashu Kharel and Ashim Gurung for their time to review this thesis for the betterment of this work, as well as Dr. Yue Zhou and Dr. Emmanuel Byamukama not only as being the part of my thesis committee member but also help to improve the quality of the thesis and upgrading the contents of this dissertation.

Equally, I can't stay without thanking Ke Chen, Rajesh Pathak, and all of the seniors PhD students for their continuous guidance towards mentoring the battery researches.

Finally, I would like to thank all the member of Dr. Qiao research group.

TABLE OF CONTENTS

LIST OF FIGURES

LIST OF TABLES

ABSTRACT

NOVEL TECHNIQUE OF FABRICATION OF POROUS COPPER AND COPPER OXIDE TO IMPROVE THE LITHIUM ION BATTERY PERFORMANCE

RAJU PRASAD GHIMIRE

2018

Due to widespread and long-term application, Lithium-ion batteries are considered as promising power sources for portable devices, satellites, medical instruments, computers, electric vehicles and grid application. It started to occupy the market once Sony commercialized in 1991. Rechargeable lithium ion batteries drawing people attention due to their peculiar properties such as high energy density and low self-discharge compared to other alkali metals. However, these widespread and long-term applications still require better batteries in terms of performance, safety and cost, which can be achieved by better utilization of anode materials and/or an optimized design of battery configuration. There are several challenges in improving the battery performance, safety and to reduce the cost. The goal of this work was to design a high-performance battery with fabricating porous current collector and copper oxide.

Current collector are essential features of batteries and being responsible for efficient charge transport to active electrode materials. In this study, a chemically treated high surface area, three-dimensional copper current collectors considerable improve the anodic performance of a batteries, by means of enhance in specific capacity and control over the fast decay. The electron transfers rapidly at the junction of the metal foam, the active material, and the electrolyte which increase the rate of redox reaction. On the other hand, the transfer of electron relatively slowly between foil current collector and the electrolyte

surface of the active material. Impedance analysis also reveals that the charge transfer resistance is lower in porous copper current collector than the non-porous one. Unique properties of porous copper current collector improve the first discharge specific capacity of $Li_2Ti_5O_{12}$ (LTO) from 168.5 $mAhg^{-1}$ to 235.8 $mAhg^{-1}$ in comparison with the non-porous copper current collector. Moreover, fabrication of binder-free copper oxide on top of porous copper can open new window to the battery research.

Chapter 1: INTRODUCTION

1.1 Background

The difficulty to meet the rapidly growing energy consumption in the world has raised concerns, with depletion energy resources and heavy environmental impacts such as ozone layer depletion, global warming, climate change, etc... Growth in population, increasing demand for building services and comfort levels, together with the rise in time spent inside buildings, assure that the increasing trend in energy demand will continue in the future[2]. Figure 1.1 shows the energy consumption forecasting until 2052[3].

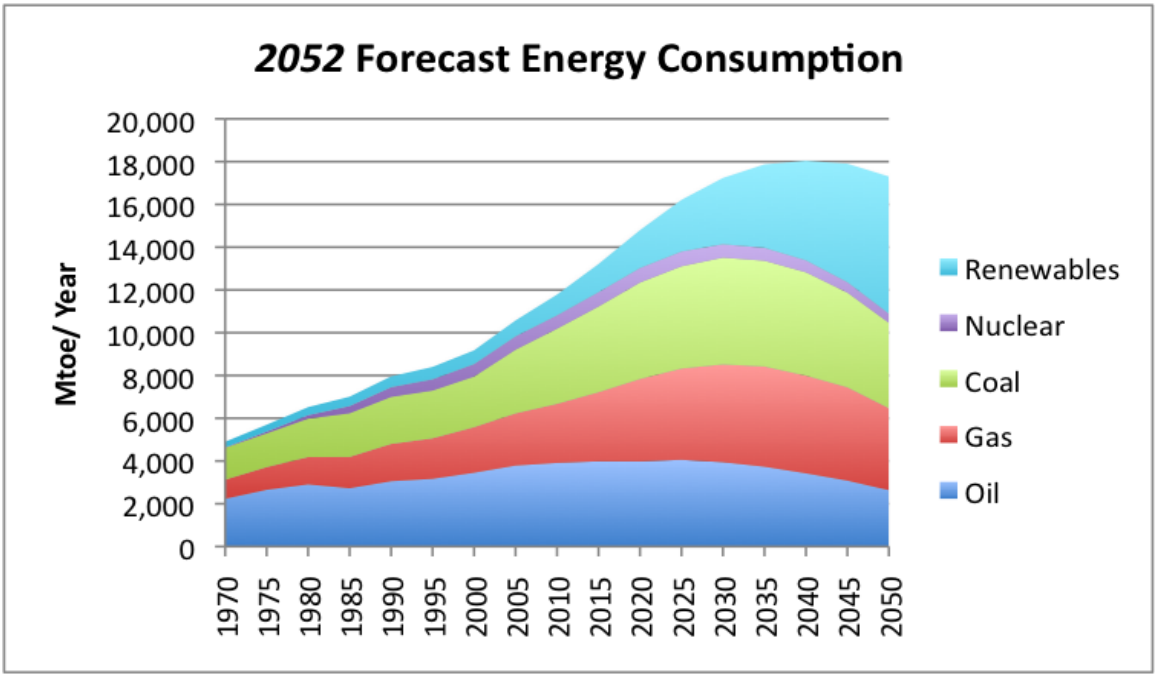

Figure 1.1 Current and future of energy consumption with economic development [2]

Current issue of the 21st century is the energy storage rather than the energy generation. Energy can be generated from the renewable energy sources such as solar, wind etc. However, these renewables cannot produce the required energy all day long. There is no sun at night and wind does not blow perpetually despite their infinite abundance. This problem can be addressed by use of energy storage which can store the solar or wind energy when available and enable the use of the stored energy later at any time when needed. Several technologies have been developed to enable energy storage such as batteries, supercapacitors, pumped hydro, and flywheel. The above-mentioned energy storage technologies offer the benefit of temporary electricity storage and using it during peak demand hours.

Energy storage devices especially batteries have been a vital part of everyday life with portable electronics. Batteries, lithium ion (Li-ion) batteries, have been monumental in the development of widespread use of portable electronics. These batteries are also being pursued for large scale energy storage applications such as electric vehicles and grid storage. In addition, energy storage plays crucial role to reduce air emissions and reduce fossil fuel usage [4]. Researcher are motivated to design a battery technology based on lithium metal as anode because Lithium is the most electropositive (-3.04 V versus standard hydrogen electrode) as well as the lightest (equivalent weight M=6.94 g mol^{-1}, and specific gravity =0.53 g cm^{-3}) metal, thus facilitating the design of storage systems with high energy

density. Figure 1.2 depicts the comparison of battery technologies in terms of volumetric and gravimetric energy density [5].

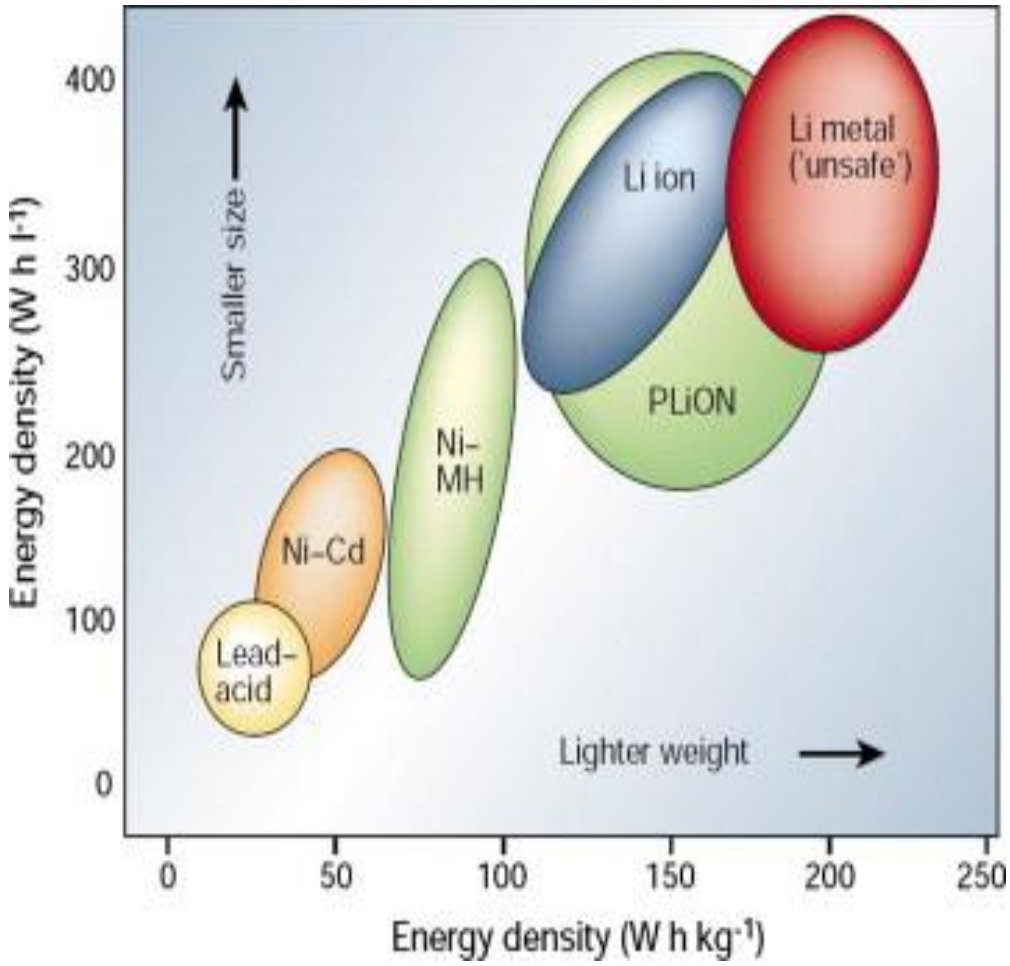

Figure 1.2 Comparison of batteries technologies in terms of volumetric and gravimetric energy density

Despite the limited source, the higher energy density makes the lithium ion batteries the most suitable for portable electronics applications. In addition, lithium is the lightest

metal and which is suitable for the portable batteries. Table 1.1 shows the Potential vs. standard hydrogen electrode (SHE) [4]

Table 1.1 Potential vs. standard hydrogen electrode (SHE) [4]

Alkali Metal	$E^0_{oxidation}$ (V vs. SHE)	ΔG^0 (kJ/mol)
$Li \rightarrow Li^+ + e^-$	3.04	293.3
$Na \rightarrow Na^+ + e^-$	2.71	261.5
$K \rightarrow K^+ + e^-$	2.93	282.7
$Rb \rightarrow Rb^+ + e^-$	2.98	287.5
$Cs \rightarrow Cs^+ + e^-$	3.03	292.0
$Fr \rightarrow Fr^+ + e^-$	2.90	279.8

The lithium ion batteries have continued to display remarkable progress in capacity, energy, power and cost reduction. Safety remains a big concern for the industry, but research and developments in new safer and stable material designs have improved the outlook for safer batteries. [6].

In a lithium ion battery, the properties of the anode and cathode materials mainly determine the specific capacity, cycle stability, and performance of the battery. With the active materials discoveries reaching a saturation stage, battery research now focuses on simpler designs and cost parameters of the existing battery components. It should be

mentioned that the lithium ion batteries are still suffering from the low power density and severe capacity fading due to structural degradation and volume change of the active materials during charging and discharging. Various researches have been carried out to address the above-mentioned issues. One of the techniques is the employment of current collectors having different structure (foil, grid, net). Figure 1.3 represent the Current battery problem [7]

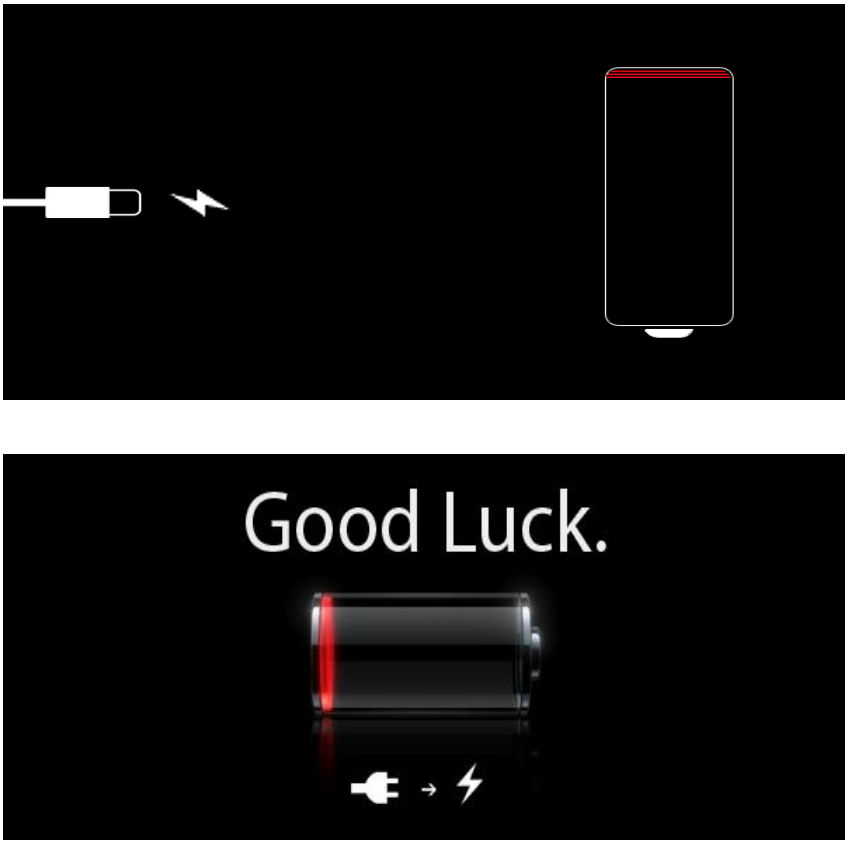

Figure 1.3 Current battery problem [7]

1.2 Literature review

As like other development, batteries also have gone through a series of journey since 17th century. For the very first time the term “battery” have been used by Benjamin Franklin in 1749 to describe the linked capacitors[7]. Figure 1.4 is a picture of the

connected capacitor[6], so called battery.

Figure 1.4 First battery configuration [6]

On the other hand, people also believed that the first battery was invented more than 2000 years ago and found while constructing a railway in 1936 near Baghdad, called Parthian Battery. Figure 1.5 shows the first Parthian battery configuration. It consisted of a clay jar that was filled with vinegar solution into which an iron rod surrounded by a copper cylinder was inserted. This device produced 1.1 to 2.0 volts of electricity when filled with vinegar[8].

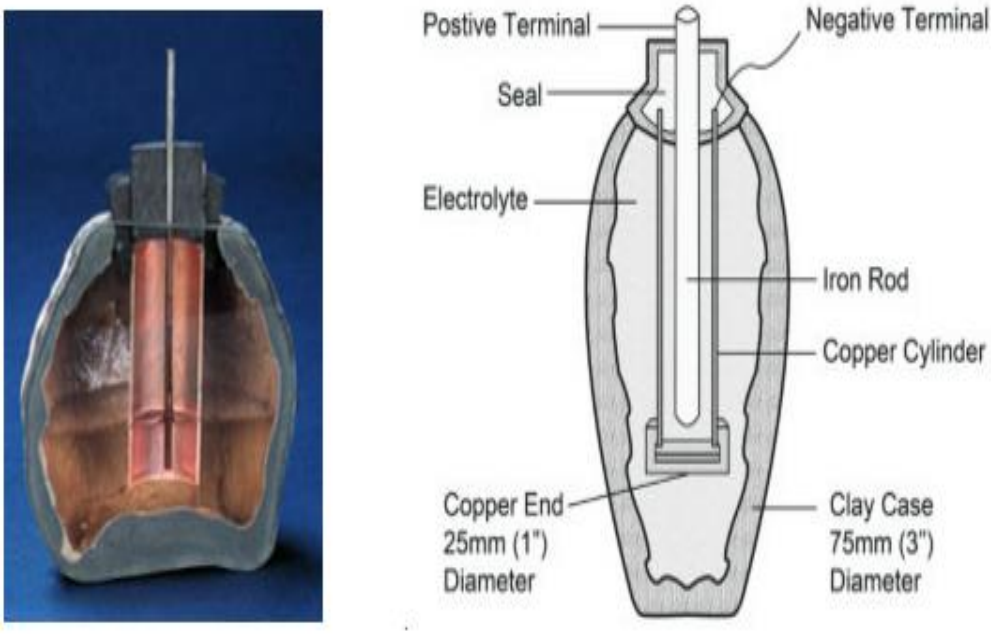

Figure 1.5 First Parthian Battery configuration [7]

With the financial supports in scientific research and investigations, researchers invested their time to develop an efficient battery which can unlock the door of advanced science and technologies. Table 2 shows the history of modern battery development. The period from 1990 to 2002 was considered as the most progressive year in the field of battery development[9].

Table 1.2 ***Summary of the History of Battery inventors with contributions*** **[8]**

Year	Inventor	Activity
1600	William Gilbert (UK)	Establishment of electrochemistry study
1745	Ewald Georg von Kleist (NL)	Invention of Leyden jar. Stores static electricity
1791	Luigi Galvani (Italy)	Discovery of “animal electricity”
1800	Alessandro Volta (Italy)	Invention of the voltaic cell (zinc, copper disks)
1802	William Cruickshank (UK)	First electric battery capable of mass production
1820	André-Marie Ampère (France)	Electricity through magnetism
1833	Michael Faraday (UK)	Announcement of Faraday’s law
1836	John F. Daniell (UK)	Invention of the Daniell cell
1839	William Robert Grove (UK)	Invention of the fuel cell (H_2/O_2)
1859	Gaston Planté (France)	Invention of the lead acid battery
1868	Georges Leclanché (France)	Invention of the Leclanché cell (carbon-zinc)
1881	Camile Alphonse Faure (France)	Invention of lead grid lattice (current system)
1899	Waldemar Jungner (Sweden)	Invention of the nickel-cadmium battery
1901	Thomas A. Edison (USA)	Invention of the nickel-iron battery
1932	Schlecht & Ackermann (Germany)	Invention of the sintered pole plate
1947	Georg Neumann (Germany)	Successfully sealing the nickel-cadmium battery
1949	Lewis Urry, Eveready Battery	Invention of the alkaline-manganese battery
1970s	Group effort	Development of valve-regulated lead acid battery
1990	Group effort	Commercialization of nickel-metal-hydride battery
1991	Sony (Japan)	Commercialization of lithium-ion battery
1994	Bellcore (USA)	Commercialization of lithium-ion polymer
1995	Group effort	Introduction of pouch cell using Li-polymer
1995	Duracell and Intel	Proposal of industry standard for SMBus
1996	Moli Energy (Canada)	Introduction of Li-ion with manganese cathode
1996	University of Texas (USA)	Identification of Li-phosphate ($LiFePO_4$)

2002	University of Montreal, Quebec Hydro, MIT, others	Improvement of Li-phosphate, nanotechnology, commercialization
2002	Group effort	Various patents filed on nanomaterials for batteries

Historically, the first battery was created by Alessandro Volta in 1880. Besides the controversy of first inventors, Alessandro Volta, being a physicist, rather than a physiologist or anatomist, concluded that it was the contact of the two-different metal that caused the frog legs to jump. After several experiments, he proposed and came up with the first functional battery called Voltaic Pile in 1800. Figure 1.6 represents the sketch of the first voltaic pile battery demonstrated by Alessandro Volta in 1801.

Figure 1.6 This image depicts an 1891 painting by Giuseppe Bertini (1825-1898) of Alessandro Volta demonstrating his battery (called the "Voltaic Pile") to Napoleon in 1801. The work is currently maintained at the Volta Temple in Como, Italy

Figures 1.7 and 1.8 shows the voltaic pile structure and working mechanism respectively. The battery consisted of zinc and copper/silver discs' pairs stacked on top of each other in which cardboard soaked in brine or a piece of cloth (current electrolyte/separator) separated the electrode layers. That battery was not a perfect battery and had some issue. The first issue was the leakage of the electrolyte due to the compression caused by the weight of the discs on the soaked cloth which in turn causes the short circuit. But, this problem by William Cruickshank two years later, by changing the device packaging from a stack of layers to a box where the layers are laid accordingly. Second issue was the short battery life due to hydrogen bubble reactions at the copper electrodes through electrolysis as well as the zinc degradation during battery operation. However, this issues only figured out later by William Sturgeon[10] coating mercury on zinc surface[11].

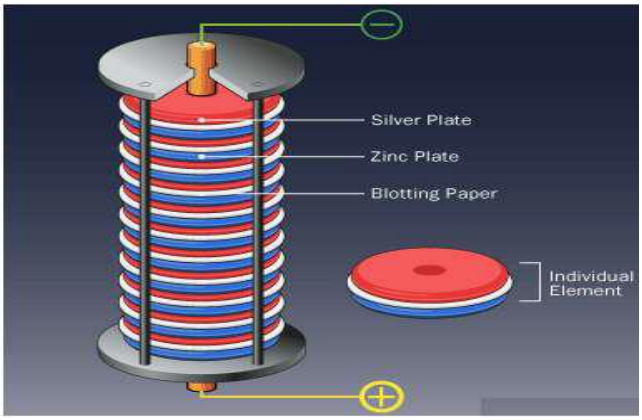

Figure 1.7 Voltaic battery, stacks of zinc and copper/silver separated by a blotting paper [10]

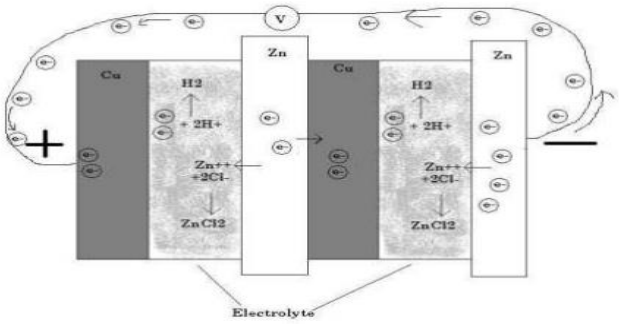

Figure 1.8 Structure and working mechanism of Voltaic Pile [10]

The issue of hydrogen bubbling was addressed by John Frederic Daniel by modifying the battery structure and arrangements, which was later considered as the first practical battery. Figures 1.9 and 1.10 show the structure and actual surviving example of the Daniell's cell respectively. The battery was made of a copper bowl filled with a solution of copper sulfate in which a smaller size porous earthenware bowl filled with a zinc plate and sulfuric acid were dipped into. The earthenware bowl acted as the separator in which only ions could pass through, but solutions did not mix with each other. The device produced 1.1 V at room temperature[12].

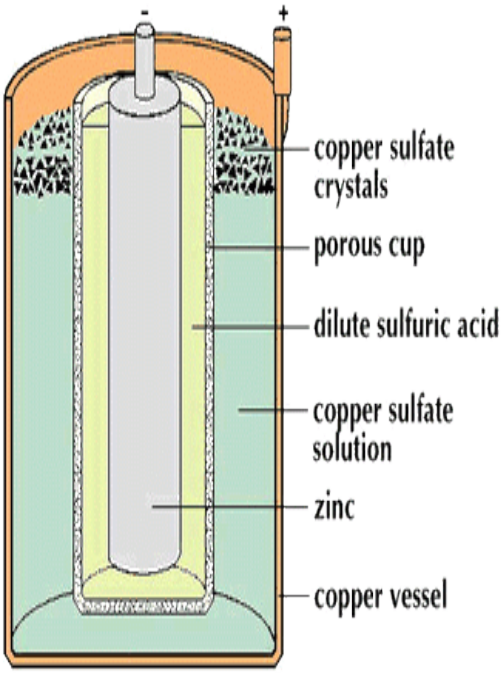

Figure 1.9 Proposed Daniell cell as the first practical battery

Figure 1.10 An actual surviving example of the Daniell cell (Jensen-Thomas) Apparatus) Collection) [10]

Daniel's cell was compromised and eventually improved to a safer model from 1837 to 1885. Later, many different prototypes such as Birds' cell, Gravity cell, Porous pot cell, Poggendorff cell, Grove cell and Dun cell were introduced. Figure 1.11 and 1.12 represent the sample structure of porous pot cell and gravity cell respectively[7].

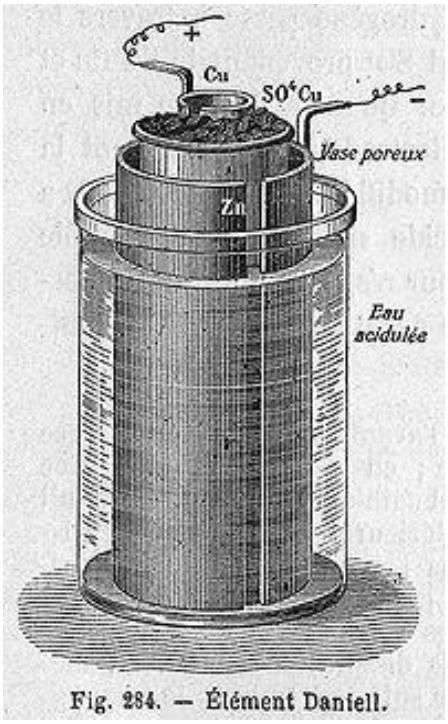

Figure 1.11 Porous pot cell

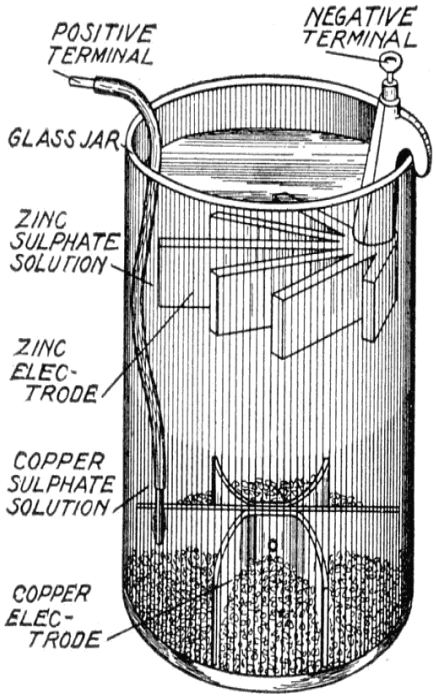

Figure 1.12 Gravity cell

Since all existing batteries would be permanently drained when all their chemical reactions were spent, Gaston Plante realized the need of a rechargeable battery and developed a lead acid battery in 1859, which is an electrochemical cell and can be recharged through passing a reverse current[13]. Beside its unique rechargeable nature, lead acid batteries were too heavy to be sufficient for multiple applications except where

the weight was not a limiting factor such as in automobiles. In 1881, Camile Alphonse Faure improved the Gaston's version of lead acid battery making it more suitable for mass production[1, 14]. Figure 1.13. shows the device structure of a Gaston's lead acid battery[15]. That lead acid cell was the first "secondary" cell.

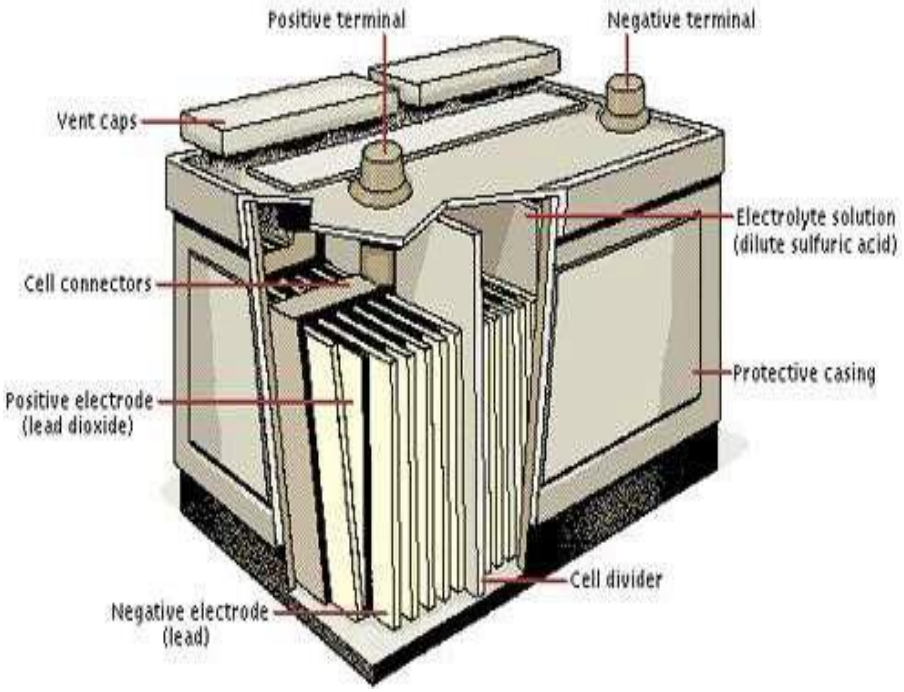

Figure 1.13: The first rechargeable Gaston's lead acid battery

Scientists, one after another, were trying to improve performance of the rechargeable battery. In 1866, Georges Leclanche invented a battery with zinc as anode and manganese dioxide as cathode wrapped in a porous material. In 1886, after 20 years, Carl Gassner designed a cell without electrolyte, a variant of the Leclanche cell, which came to be known as the dry cell. In a similar way, first alkaline battery Nickel Cadmium (NiCd) with nickel as a positive electrode and cadmium as negative electrode in a potassium hydroxide solution as electrolyte, was invented by Waldemar Jungner in 1899[16]. People were

looking for a battery with high energy density and lighter weight and NiCd seemed more promising than the lead acid battery at that time.

Thomas Edison solved some minor issues about Jungner's nickel-iron battery and commercialized it in 1903. A lighter weight version of Gaston's lead acid battery was proposed by Edison which had a great advancement for electric and diesel-electric rail vehicle applications. Until 1959, much progress on primary (non-rechargeable) cells have been made; and zinc carbon and later zinc-manganese dioxide batteries based on alkaline electrolyte entered the market[16]. Figure 1.14 shows an alkaline primary battery- zinc-carbon battery[17].

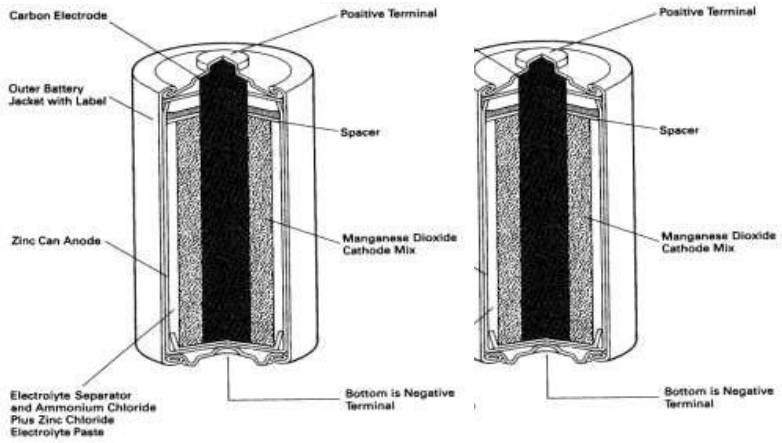

Figure 1.14 Commercialized zinc-carbon battery, an alkaline primary battery [18]

As described earlier, lithium possesses the combination of lowest density and highest electrochemical potential After 1980, major discoveries of $LiCoO_2$-cathode by John B. Goodenough, graphite-anode by Rachid Yazami led to the demonstration of the first lithium-ion battery in 1985 and was fabricated by Akira Yoshino. Ultimately, Sony

commercialized the lithium-ion battery in 1991[10, 18-20]. However, no new major battery system has entered the commercial market since the invention of Li-phosphate in 1996.

The superior energy density enabled the lithium ion batteries to provide the same amount of energy as other battery chemistries with a much smaller volume or weight. Therefore, since the invention to present day, lithium ion batteries have been revolutionary in portable electronics and are being heavily investigated for electric vehicles and grid storage applications. Numerous applications are now increasing the demand for batteries with much higher energy density and faster rate performance. In recent years, much effort has been made to identify the new materials and enhance the capacity[21].

1.3 Previous work

In 1990, Debra Rolison et al.[22, 23] designed the first porous internal architecture of a device which can be used as a catalyst in sensors. That technique allowed people to use porous lead in lead acid battery and they found the mechanical and electrical properties are convenient for high current. By considering the above phenomenon of porous structure, there has been a great interest in designing porous metals.

The research on foamed and porous metallic materials has become an attractive research field since they exhibits many unusual combinations of physical and mechanical properties, such as permeability of air and water, impact energy absorption capacity, unusual acoustic energy absorption ability, and lower thermal conductivity, etc [24]. Various fabrication techniques have been used to prepare porous copper such as dealloying, powder sintering, electrochemical deposition, solid-gas eutectic solidification method,

casting, and templates [25-28]. Most of the above-mentioned processes are complex, demanding and the preparation cost is too high.

As mentioned above porous metals containing a large number of pores shows various characteristics such as large specific surface area and low density, which are different from those of bulk metals[29, 30]. Porous metals are not only lightweight and high-strength, but also multifunctional. These include many special properties including shock damping, acoustic absorption, heat dissipation, electromagnetic shielding and high electrical conductivity [31-34].

Formation of porous copper has been the subject of many investigations for the past few decades. Copper containing several pores has been studied for different industrial applications. Porous copper having large specific surface area, high electrical conductivity and other special functionalities[35-40] make copper a specialized product for applications in separation systems, sensors, batteries, fluid flow control, self-lubricating bearing, catalysts and electrochemistry. Moreover, the porous metals with different porosity and structure may be synthesized for filters, metal-matrix composites, brakes, and damping elements, etc[41] Because of its special porous structure and novel physical and mechanical properties, porous copper is widely studied in many fields, as catalyst, separator, sensor, &especially in high-performance lithium-ion batteries[42-47]. In 2o16, Liu et.al summarize the preparation techniques of porous copper for Lithium-Ion battery application. These includes Casting, Powder Metallurgy (PM), Dealloying and Electrodeposition. However, these methods have their own limitations. Casting and Powder Metallurgy techniques required a high temperature (800-1300^{o}C) and pressure (0.2-300MPa). On the other hand, the corrosive chemicals have been used in Dealloying method. The porous copper fabricated by these methods have low porosity (< 80%) and

bigger pore size (several hundreds of μm) in comparison with electrodeposition[48]. Fabrication of porous copper using electrodeposition technique usually occurs under electric potential or current density with gas bubbles as dynamic templates [49, 50]. The electrodeposition technique has been used, since it is a simple and rapid method for preparing porous and reticulated Cu films with small pore size (in several tens of μm) high porosity (80–99%), and thin thickness (in several tens of μm)[45-47]. Compared with traditional fabrication techniques, electrodeposition method has attracted much attention due to its comprehensive advantages of low cost but still required to heat the sample in many cases. But anodization technique using glycerol, DI water and sodium bicarbonate has not been reported yet.

Unlike the planner copper, porous copper improves adhesion of the active material [51, 52], and accommodate strain occurring during the lithiation-delithiation reaction[53-55] . Porous current collectors also accelerate surface electrochemical reactions[56, 57] and lithium ion transport[57]. Porous copper current collectors are also well known for their chemical compatibility with battery electrolytes and ability to improve the cycle performance of LIBs[58-60]. However, there are some challenges in using porous metal as current collector for Li-ion batteries because conventional porous metal generally have low tolerance during charging or discharging, especially at high voltages and preparation cost also too high, but porous copper is particularly interesting in this respect, due to its relatively low cost and convenient mechanical/electrical properties for high currents[61, 62]. Additionally, the porous metal should not react with any active materials or electrolytes during charging and discharging[63, 64] and the porous copper does not have any side reaction with other chemicals used in LIB.

High surface area porous copper current collectors considerably improve the performance of cathodes and anodes in batteries, but their technological implementation is impeded by the complexity of their preparation, which needs to be simple, fast, and energy efficient. An alternative, innovative, simple and environmental friendly method need to be developed to fabricate porous copper using anodic oxidation. Pores on copper were achieved by anodically oxidizing copper using an electrolytic solution under an electric potential. The chemically treated porous copper has a porosity of 81.8% and a high specific area. Use of porous copper as current collector not only facilitates the redox reaction with shorter electron and lithium ion transfer length by providing a high specific area, but also allows the construction of a lightweight battery. This makes porous copper very attractive current collector for Li-ion batteries.

Another remarkable discovery by Tarascon's group in 2000[65-67] was the transition metal oxide as the anode materials for the lithium ion batteries since they have higher capacities (600-1000 mAhg-1). However, the transition-metal oxide is beset by formidable technical difficulties such as charge transfer limitations associated with poor kinetics that results mainly from interfacial phenomena between active materials and current collectors[68-70]. The poor kinetic process and electrical conductivity can affect conversion reactions of transition-metal oxides with lithium resulting in the large polarization, the low energy efficiency and the poor cycle performance[71, 72]. To fully utilize the concept of conversion reactions for the manufacture of high performance lithium ion batteries, it is challenged to create an advanced electrode design/configuration[68]. For the traditional casting-derived electrode[73-75] ,transition metal oxide electrodes usually

have some difficulty to maintain their close contact with current collectors over several tens of charge/discharge cycles[76].

Recently, metal oxides have been extensively studied as ideal components for the electrode materials of LIBs with significantly theoretical capacity[66, 77-80]. In particular, CuO has drawn considerable attention with high theoretical capacity (674 mAhg-1) than commercial graphite (372 mAhg-1), low cost, high safety and environmental friendliness[67, 81]. However, CuO suffering from the unavoidable huge and uneven volume expansion (about 174%) lead to the degradation, cracking and pulverization of the electrode material, which results poor capacity retention and dramatic capacity loss[82]. Several efforts have been focused on the optimization of electrode designs for efficiently marrying current collectors with transition-metal oxide anode materials[68, 69, 71, 83, 84]. The configuration of nanoarchitecture electrodes has been an effective route to overcome above-mentioned drawbacks. In this regard, various types of CuO nanostructures have been exploited for lithium ion electrode materials[85-89],which propose that the nanoscale microstructure provides a large free space to allow fast Li ion across the interface and releases the large volume variation during the Li insertion and extraction process, resulting in the suppression of electrode material degradation[90]. But, Jun Li et al. in 2017 put their effort to generate copper oxide on top of the porous copper and achieve higher capacity (940 mAhg-1) for the first discharge, which is higher than reported before[90]. However, in situ generation of copper oxide on top of porous copper through anodization has not been done before.

1.4 Motivation

Fabrication of an efficient current collector and binder free copper oxide on top of porous copper, by using a novel, convenient, scalable, efficient, cheapest and environmental friendly way to enhance performance of energy storage device like the specific capacity of LIB at different charging/discharging current rate.

1.5 Objectives

The major objective of this research work was to enhance the performance of the lithium-ion battery by using porous copper current collector and binder free copper oxide as battery anode to accomplish the mentioned objectives, the following tasks were performed:

1) Optimize the anodization parameters for copper oxidation.

2) Fabricate and optimize pores on copper foil substrate by anodization.

3) Fabricate the copper oxide by heating after anodization.

4) Fabricate Li-ion half-cells using porous and planner current collector with lithium titanite electrode and investigate charge/discharge performance.

5) Fabricate Li-ion half-cells using electrodeposited copper oxide as potential anode and investigate charge/discharge performance.

Chapter 2: THEORY

Battery

Battery is an electrochemical device that converts chemical energy to electrical energy. A battery consists of a multiple number of electro chemical cells. Major attributes of a battery include its capacity, durability, charging time, safety, toxicity and cost which determine the battery market. There are two kinds of battery available: non-rechargeable (Primary) and rechargeable (Secondary) batteries. Primary Batteries are designed to be used until the energy is exhausted and need to be replaced with a new one. Their chemical reactions are not reversible but can be used immediately after the fabrication. However, secondary batteries can be recharged since their chemical reactions are reversible but are required to be charged before use[91]. Brief examples and comparisons of primary and secondary batteries as follows: Table 2.1 and 2.2 shows the list and comparative study of primary and secondary batteries.

Table 2.1 List of Primary and Secondary Batteries

Primary	Secondary
Alkaline battery	Flow battery
Zinc-carbon battery	Fuel cell
Bunsen cell	Lead acid battery
Atomic battery	Lithium-air battery
Molten salt battery	Lithium-ion battery
Chromic acid cell	Nickel-cadmium battery
Nickel oxyhydroxide battery	Polymer based battery
Clark battery	Sodium ion battery
Mercury battery	Magnesium-ion battery
Weston battery	Molten salt battery
Zamboni battery	Silicon-air battery
Daniell cell	Sodium/Lithium-sulfur battery

Table 2.2 Comparative study of primary and secondary batteries [15]

Type	Cost Effectiveness	Performance	Safety and Environmental Effects	Applications
Primary	Cheaper individual batteries but must be replaced after every discharge	Higher energy density, initial voltage and capacity	Producing toxic wastes and minerals and mostly non-recyclable such as non-rechargeable AA,AAA,C and D cells	Watches, electronic keys, flashlights, toys, military devices in combat
Secondary	Rechargeable	Lower energy density, initial voltage and capacity compensated by its significantly longer life time in terms of energy supplement	Almost non-hazardous wastes, but heavy metals such as Lithium and Lead must be recycled.	Telecommunication, portable electronics, electric vehicles, starting and ignition of cars, emergency power supplies and etc

2.1 Secondary Batteries

Rechargeable batteries play an important role in our lives and many daily chores would be unthinkable without the ability to recharge the batteries. The most common rechargeable batteries are lead acid, Nickel Cadmium (NiCd), Nickel metal hydride (NiMH), and Li-ion. Current research also shows significant results from other battery technologies such as sodium-air, sodium-ion, lithium-air, solid state batteries and so on but are in research and development stage.

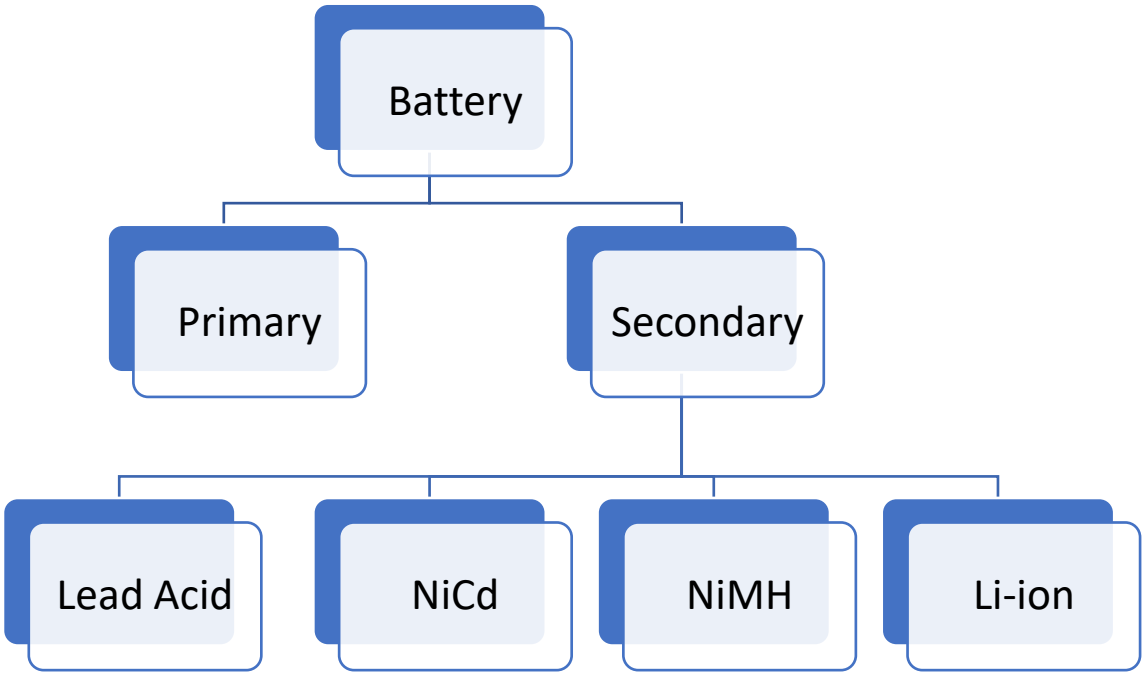

Figure 2.1 List of secondary batteries

2.1.1 Working principle of Lead acid battery

Lead acid battery was the first rechargeable batteries where lead, lead dioxide and sulfuric acid was used as anode, cathode and electrolyte respectively. Low specific energy, environmentally hazardous, slow charge/discharge and limited cycle life are the issues with

lead acid t battery. However, lead acid batteries are cheap to manufacture, has high specific power, good performance at low temperature and excellent performance at high temperature and low self-discharge as well. After the year 2009, almost all the lead acid batteries are being recycled. Figure 2.2 shows the charging and discharging processes of lead acid battery[92]..

The chemical reactions that occurs inlead acid battery can be written as:

$Pb(s) + HSO^-_4(aq) \rightarrow PbSO_4(s) + H^+(aq) + 2e^-$ [at Anode]

$PbO_2(s) + HSO^-4(aq) + 3H^+(aq) + 2e^- \rightarrow PbSO_4(s) + 2H_2O$ [at Cathode]

$Pb(s) + PbO_2(s) + 2H_2SO_4(aq) \rightarrow 2PbSO_4(s) + 2H_2O(l)$ [Overall reaction]

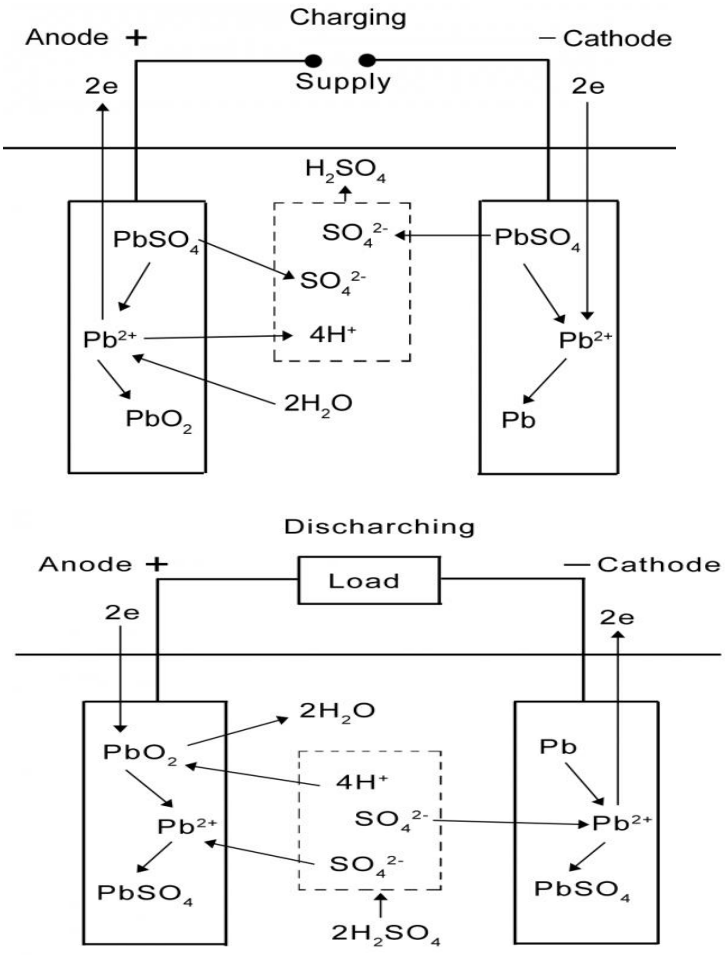

Figure 2.2 Charging (upper) and Discharging (lower) at lead acid battery [48]

2.1.2 Working principle of Nickel-Cadmium battery

Nickel based batteries (Nickel-Cadmium, Nickel-Iron, Nickel-Hydrogen, Nickel-Zinc and Ni-metal hydride) started developing to address the limitations of the lead acid batteries. Nickel-Cadmium (NiCd), first alkaline battery, is one of the most rugged and enduring batteries and has long service life. Because of the toxic nature of Cd in NiCd batteries, it is being replaced with other chemistries, but it retains its status in aircraft due to its good safety records. Figure 2.3 shows the structure of NiCd battery.

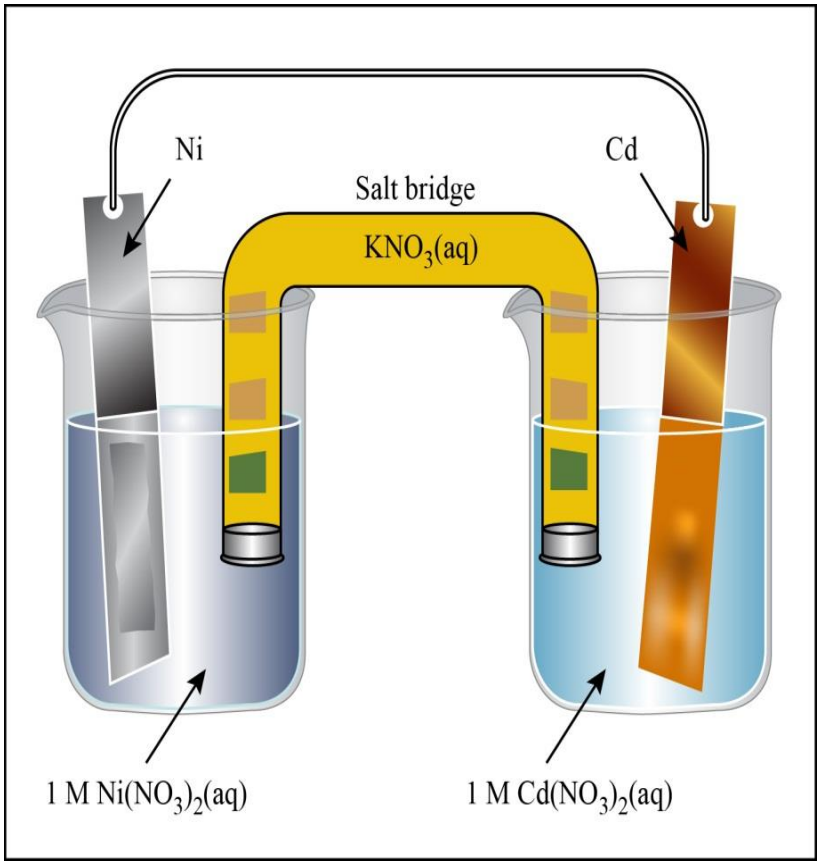

Figure 2.3 Nickel Cadmium battery schematic diagram

Chemical reactions that occur in nickel-based battery can be written as:

$NiO(OH) + 2H_2O + 2e^- \rightleftharpoons 2Ni(OH)_2 + 2OH^-$ [at cathode] ----------$Eq^{n.}$ (1)

$Cd + 2OH^- \rightarrow Cd(OH)_2 + 2e^-$ [at anode if cadmium is anode]

In above equation (1), the nickel (III) oxide-hydroxide NiO(OH) which has been the active material of the cathode will produce $Ni(OH)_2$ as a product of the discharge. Similarly, during the charge or preferably recharge process, the NiO(OH) will be reconstituting in the presence of the water again. As lead acid battery, nickel based battery's reactions happen in an aqueous environment as well[93]. However, the alkaline electrolyte is not consumed in recharge reaction, which lead to higher cell stability since the state of charge is not determined by the specific gravity of the electrolyte.

Nickel based batteries have fast charge/discharge rate compared to other secondary batteries. It also has mechanically robust structure, excellent performance at low temperature. In addition, in terms of price per cycle, NiCd can be considered as the cheapest and has long life and can be stored in discharged state as well. However, Nickel based batteries suffer from memory effect, high discharge rate in unused condition and has low open circuit voltage and low specific energy as well[13, 94, 95].

2.1.3 Working Principle of Lithium-ion Battery

In lithium ion battery, metal oxide works as cathode and carbon-based material typically graphite works as an anode and electrolyte is a lithium salt dissolved in an organic solvent. The two electrodes are separated by a polymer separator membrane for electrical

isolation but the membrane is ionically conducting[49]. Discharge of a battery happens by oxidation of anode or reduction of cathode and reverse happens during charging. Variety of materials can be employed as electrodes in lithium ion batteries and different performance level can be achieved. Figure 2.4 shows the ion flow mechanism in Lithium ion Battery and Figure 2.5 shows the charging and discharging mechanisms of a full cell lithium ion battery.

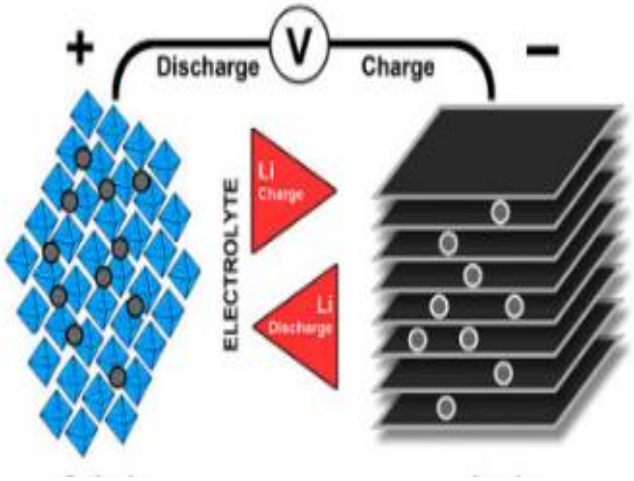

Figure 2.4 Ion flow in lithium-ion battery [49]

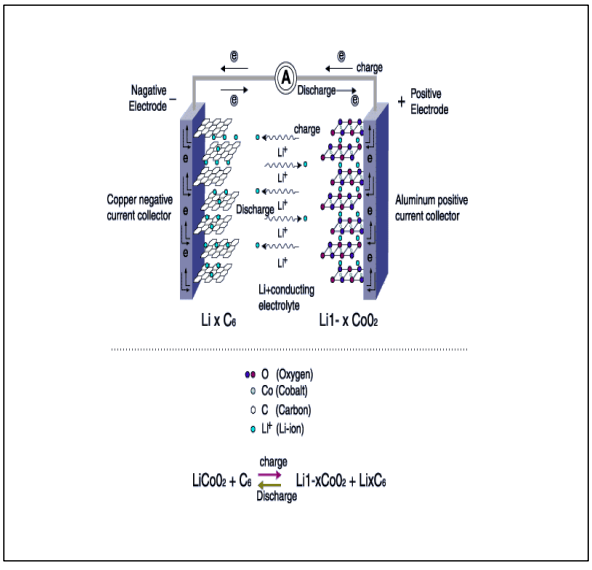

Figure 2.5 Charging and discharging reaction of full cell lithium ion battery

The chemical reactions taking place in lithium ion battery can be written as:

During Charge:

$LiCoO2 \rightarrow Li_{1-x}CoO2 + xLi + + xe^{-}$

$6C + xLi + + xe - \rightarrow LixC6$

During discharge:

$Li_{1-x}CoO2 + xLi + + xe^{-} \rightarrow LiCoO2$

$$LixC6 \rightarrow 6C + xLi + + xe -$$

Regarding to the reaction mechanism, only six carbon atoms can bind one lithium ion. To improve the performance of a lithium ion battery, an efficient anode material is required which can hold more and more lithium ions. Several materials have been tried but there is a huge interest in silicon because one silicon atom can hold 4 lithium ions. Theoretically, silicon electrodes can store over 10 times than that of graphite. The lithium ion battery is known as a rocking chair battery due to charge carriers shuttling back and forth between two intercalating electrodes during the charge and discharge processes[96]. Table 2.3 summarizes the pros and cons of lithium ion batteries.

Table 2.3 AAdvantage's and disadvantages of Lithium ion batteries [1]

Advantage	**Disadvantage**
High specific capacity, cycle durability and columbic efficiency	Degrades at very high or very low temperature; best performance in 0-45◦ C
High specific energy per unit weight	Thermal runaway if the cell is stressed; protection circuit needed
Very low self-discharge rate	Transportation of large quantities are subjected to the safety regulations
More simple charge and discharge process compared to other secondary batteries	Electrode and electrolyte material are changing on a continuous trend
Long life cycling with minimum degradation; easy maintenance	Expensive manufacturing process; almost 40% NiCd

During the charging and discharging process of a Li-ion half-cell, where LTO used as cathode and lithium metal foil used as reference anode, the following reactions take place: During discharge (lithiation): $Li_4Ti_5O_{12} + 3Li^+ + 3e^- \rightarrow Li_7Ti_5O_{12}$

During charge (delithiation): $Li_7Ti_5O_{12} \rightarrow Li_4Ti_5O_{12} + 3Li^+ + 3e^-$

During lithiation, the lithium metal is oxidized liberating Li ions into the electrolyte and electrons into the external circuit. These Li ions diffuse towards the cathode where lithium titanate is reduced. During delithiation, the reverse happens and is accomplished using

external field. The theoretical capacity of active material can be calculated by the given equation with lithium titanate as an example:

$$\frac{F \cdot x}{M} = \frac{96458.3\ C/mol}{459.09\ g/mol} \times 3 = 630.32\ C/g = 175.57\ mAh/g$$

Where, F = Faraday constant = 96458.3 C/mol

x = Number of electrons transferred per unit = 3

M = Molecular weight of active material

= 6.941*4+47.867*5+15.9994*12 = 459.09 g/mol

2.2 Battery Terminologies

The parameters that define the performance of a battery are:

- **C- and E- rates**: A C-rate is a measure of the rate at which a battery is discharged relative to its maximum capacity. A 1C rate means that the discharge current will discharge the entire battery in 1 hour. A C-rate of 1C is also known as a one-hour discharge; 0.5C or C/2 is a two-hour discharge and 0.2C or C/5 is a 5-hour discharge. For example, if the battery has a capacity of 500Ah (Ampere-Hour), the discharge current of 500A will be needed to fully discharge this battery in one hour at 1C rate. Some high-performance batteries can be charged and discharged above

1C with moderate stress. Similarly, an E-rate describes the discharge power. A 1E rate is the discharge power to discharge the entire battery in 1 hour.

- **State of Charge (SOC) (%)**: It is an expression of the present battery capacity as a percentage of maximum capacity. SOC is generally calculated using current integration to determine the change in battery capacity over time.
- **Depth of Discharge (DOD) (%):** It is the percentage of battery capacity that has been discharged expressed as a percentage of maximum capacity. An 80 % DOD is referred to as a deep discharge.
- **Open-circuit voltage (V):** It is the voltage between the battery terminals with no load applied. The open-circuit voltage depends on the battery's state of charge and increases with state of charge.
- **Internal Resistance (Ω):** It is the resistance within the battery, generally different for charging and discharging, also is dependent on the battery state of charge. As internal resistance increases, the battery efficiency decreases and thermal stability is reduced as more charging energy is converted into heat.
- **Cut-off Voltage (V):** It is the minimum allowable voltage that generally defines the "empty" state of the battery**.**
- **Specific Capacity (Ah/kg):** The specific capacity is the product of constant discharge current (A) and the time it takes to discharge (h) per weight of the active material in battery electrode (kg). It basically defines the amount of charge the battery can hold.
- **Specific energy (Wh/kg):** The specific capacity is the product of discharge power

(W) and the time it takes to discharge (h)per weight of the active material within battery electrode (kg). It basically defines how long the battery will last.

- **Specific power (W/kg):** This parameter is the ratio of the available power to the weight of the active material within anode electrode (kg). It basically defines how fast the battery can be discharged.
- **Charge Voltage (V):** The voltage that the battery is charged to when charged to full capacity. Charging schemes generally consist of a constant current charging until the battery voltage reaching the charge voltage, followed by constant voltage charging, which decreases the charging current to a set value.
- **Float Voltage (V):** The voltage at which the battery is maintained after being charge to 100 %SOC to maintain that capacity by compensating for self-discharge of the battery.
- **Nominal Voltage (V):** The reported or reference voltage of the battery, also sometimes thought of as the “normal” voltage of the battery[97].

2.3 Principle of Current Collectors

In batteries research, current collectors also play a significant role for the battery performance. Selection of current collectors is based on two characteristics: (a) Electronic conductivity and (b) Potential stability. For the half-cell of lithium ion battery, the working potential for anode is about 0.5V to 2.5V and as anode copper (Cu) has oxidation potential of 0.337V with respect to hydrogen and about 2.7V with respect to lithium. So, copper is suitable for anode material. On the other hand, the working potential for cathode is about

3.0V to 4.7V and aluminum (Al) has an oxidation potential of 1.662 V with respect to hydrogen and about 4.7 with respect to lithium. Nickel is also stable for anode current collectors like copper but nickel is expensive. If the potential does not match, side reactions occur and stability cannot be achieved at desired level[98].

2.4 Porous Copper Formation

Porous copper is a network of copper crystals having voids. There are four well-established techniques which can be used to fabricate porous copper such as casting, powder metallurgy, dealloying, and electrodeposition[48].

Figure 2.6 Copper metal

Casting is done by passing the high-pressure gases (hydrogen and argon) of 0.2-2 MPa into the melted copper at a high temperature of 1200-1300°C followed by waiting until it solidifies. Pores in copper can be found due to the solubility gap of the gases between liquid and solid[99]. The orientation, size, and density of the pores in the porous copper can be controlled by gas pressure, freezing direction, solidification velocity, transfer velocity, melting temperature etc.[29, 99-101].

Powder metallurgy is the technique to make porous copper by foaming during the sintering process after blending and compacting of raw materials containing Cu powders and foaming agents[27]. The orientation, pore size, porosity, morphology and mechanical properties of porous copper depends on the sintering time, sintering temperature, compaction pressure, and the amount, time, and size of the foaming agent. Pore obtained

by this technique has porosity of 50-85% and pore size is 53-1500 micrometer. The required pressure (75-300 MPa) and sintering temperature (800-1000^{o}C)[35, 102].

Dealloying occurs under driving force when alloys are immersed into electrolyte, so that more reactive components are chemically or electrochemically etched owing to them high reactivity, but noble components remain stable in the metallic form. Despite its high pollution causing characteristic owing to the use of corrosive chemicals and contamination by other compositions, dealloying is an effective way to prepare Cu films with the pore size of several hundreds of nm (even down to several tens of nm) and certain thickness[103-107].

Electrodeposition usually occurs under applied current density or electric potential with gas bubbles as dynamic templates[49, 50]. The distribution, number and pore size explicitly depends on the potential or current density and time and they are also affected by concentrations of copper ions, temperature and composition of working electrodes[30, 38, 42, 45, 47, 101]. Porous copper fabrication using the electrochemical anodization technique is a well-known technique, which uses the galvanostatic condition. This technique renders a wide range of porosity and thickness. For electrochemical etching of copper, copper substrate is placed in an etching cell consisting of electrolyte and a counter electrode. Separation between copper and the counter electrode in maintained at certain distance and the external bias is applied.

2.5 Copper Dissolution

Porous copper formation involves two simultaneous reactions: oxidation and dissolution of copper, which require valence band holes be driven to the surface under depletion condition. The exact mechanism by which the pore forms in copper substrate has

not been satisfactorily explained and several mechanisms have been proposed. The pore morphology, size and number depend on the applied current, voltage, electrolyte composition and oxidation time. Availability of valence band holes is the most important factor for pore formation, which is primarily determined by the dopants, glycerol-based electrolyte concentration and applied electric field. It has been believed that initially the copper surface is passivated with hydrogen. It is explained by the evolution of hydrogen gas during the process of electrochemical etching of copper and hole requirement for the dissolution to occur. The constant current of 0.20 A applied for 10 mins on the copper foil forms a layer of $CuCO_3$ via nucleation and growth from solution. The dissolved Cu^{2+} ions that are needed for the precipitation of $CuCO_3$ are produced from the metal dissolution that results in the formation of pores on the copper surface. However, the surface is fully passivated by $CuCO_3$ [108]. Figure 2.7 and figure 2.8 shows the copper sample after anodization and the mechanism of pore formation during anodization.

The overall reaction during the oxidation is

$$C_3H_8O_3 + 3H_2O + NaHCO_3 + Cu \longrightarrow CuCO_3 + 3CO_2 + NaOH + 14H^+ + 14e^-$$

Figure 2.7 Copper sample after anodization

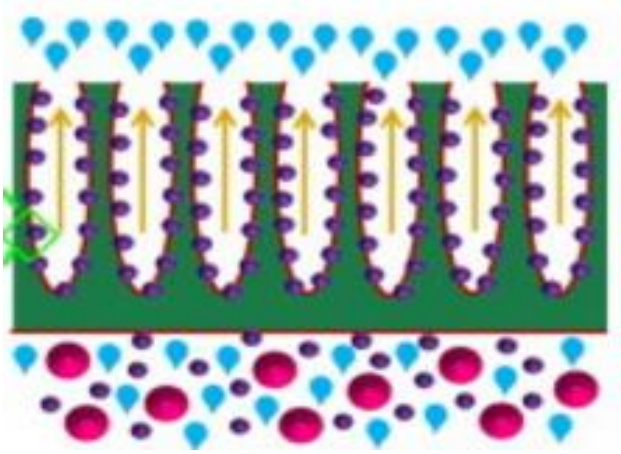

Figure 2.8 Mechanism of pore formation during anodization

2.6 Copper Oxide Fabrication Technique

Copper oxide can be formed by heating the copper carbonate once copper carbonate is deposited to the copper after the anodization. The chemical reaction can be written as:

$$CuCO_3 \longrightarrow CuO + CO_2$$

Chapter 3: EXPERIMENTAL PROCEDURE

3.1 Materials and Crystal Structure

Fabrication of lithium ion battery using porous copper as a current collector involved several steps, materials and characterization. Materials like Copper, DI water, Soap, Acetone, Glycerol, Sodium bicarbonate are required to fabricate the porous copper. Battery fabrication was done by using $Li_4Ti_5O_{12}$ (LTO >98%, MTI), which contains 90% of the particle are less than 4.24 μm, was used as an anode material (AM), pure Li metal foil (99.9%, MTI Corp) as a cathode (C), Polyvinylidene fluoride (PVDF) as a binder (B), Super Carbon as a conductive agent (CA), N-methyl pyrrolidone (NMP) as a solvent and Lithium perchlorate as an electrolyte.

3.1.1 Copper

The used copper (Purity > 99.99% and Density 8.94 $g.cm^{-3}$) foil for battery anode substrate was from MTI corporation. One side of the foil was polished and thickness of the copper foil was 9μm. Figure 3.1 shows the picture of copper foil used for oxidation and finally as a battery substrate.

Figure 3.1 Roll of copper foil

3.1.2 Glycerol and Sodium Bicarbonate

The chemical formula for glycerol is $C_3H_8O_3$ as shown in Figure 3.2. It was used as an oxidizing agent (electrolyte for the electrolysis). Pure glycerol (> 99.1 %) from the HACH has been used. Sodium bicarbonate ($NaHCO_3$), as shown in Figure 3.3 is also known as baking soda and was used as a conductive agent during the electrolysis.

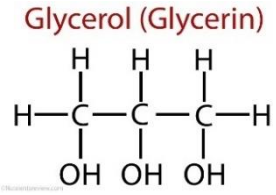

Figure 3.2 Glycerol Structure

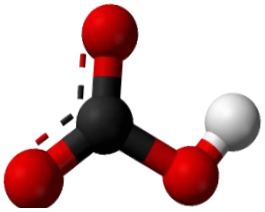
Figure 3.3 Sodium bicarbonate structure

3.1.3 Lithium Titanium Oxide

It is also known as Titanate (LTO), Li4Ti5O12 as shown in Figure 3.4, (Purity >98%, MTI), which contains 90% of the particle are less than 4.24 μm and 10% of the particles less than 1.09 μm, was used as an anode material in a Li-ion half-cell.

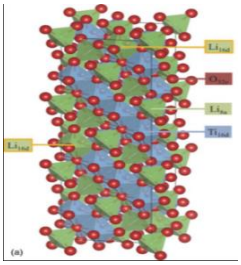
Figure 3.4: Titanate Structure

3.1.4 Polyvinylidene fluoride

Generally, it is known as a PVDF (Purity > 99.5%) from MTI corporation. The chemical formula is $-(C_2H_2F_2)_n-$ as shown in Figure 3.5. It was used as a

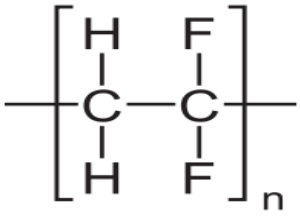

Figure 3.5: PVDF Structure

binder for the Li-ion cells. It contains moisture less than 0.1%.

3.1.5 N-Methyl-2-pyrrolidone

The chemical formula is C_5H_9NO as shown in Figure 3.6, mostly called NMP. The molecular weight is 99.134 and has purity more than 99.5%. During the experiment, it was used as a solvent for PVDF.

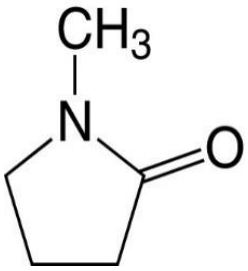

Figure 3.6 NMP Structure

3.1.6 Super P Carbon

Timcal super C45 conductive carbon black as shown in Figure 3.7 was used as a conductive additive. The size of spherical particles is called "particle size," and the size of the particle chain is called "structure." Various functional groups such as the hydroxyl or carboxyl group are found in the surface of carbon black.

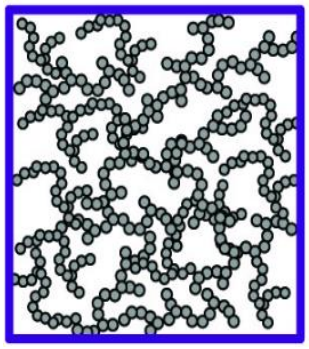

Figure 3.7 Super Carbon Structure

3.1.7 Copper(II) Oxide (CuO)

Copper oxide is a black solid and inorganic compound also known as cupric oxide with structure shown in Figure 3.9. CuO was formed by thermally heating of copper carbonate after the anodic oxidation of copper.

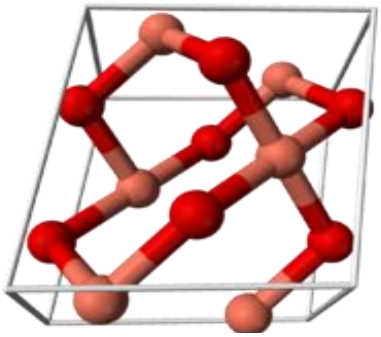

Figure 3.8 CuO Structure

3.2 Fabrication Procedure

3.2.1 Porous Copper and Copper Oxide Formation

Pore on copper was formed by anodic oxidation of copper using electrolytic solution under electric potential. First, sample measuring 2.5 x 5 cm were cut from Cu foil and cleaned with warm soap water. Cleaned sample were ultra-sonicated for 15 min each in (a) deionized (DI) water (b) acetone and (c) isopropanol. Electrolyte solution was prepared using 1:2 volume ratio of DI water and glycerol along with 1 at. wt. % of sodium bicarbonate and the solution was stirred for an hour by using magnetic stirrer.

Galvanostatic anodization was performed in a metal beaker. Copper electrode connected to the positive terminal of the power supply as anode and negative terminal was connected to the beaker itself. Power supply was used to supply the potential. Anodization was carried out in constant current mode at different current range from 0.01 A to 2.00 A. To form a regular pore on copper surface the constant current of 0.20 A was applied for 10 min. Various parameter of the anodized sample was studied and best sample was used for the fabrication process.

Figure 3.9 shows the Schematic diagram of fabrication procedure of porous copper and copper oxide. Porous copper was obtained by ultrasonicating the anodized samples in isopropanol for 60 minutes to remove the green layer of copper carbonate. On the other hand, copper oxide was obtained by heating the copper carbonate instead of ultrasonicating the samples. The heating of the copper carbonate was done in the atmosphere at the temperature of 200^{o}C for 10 minutes over the hotplate. Figure 3.10 Anodic Oxidation Copper Sample(a) Schematic diagram (b) Laboratory Setup.

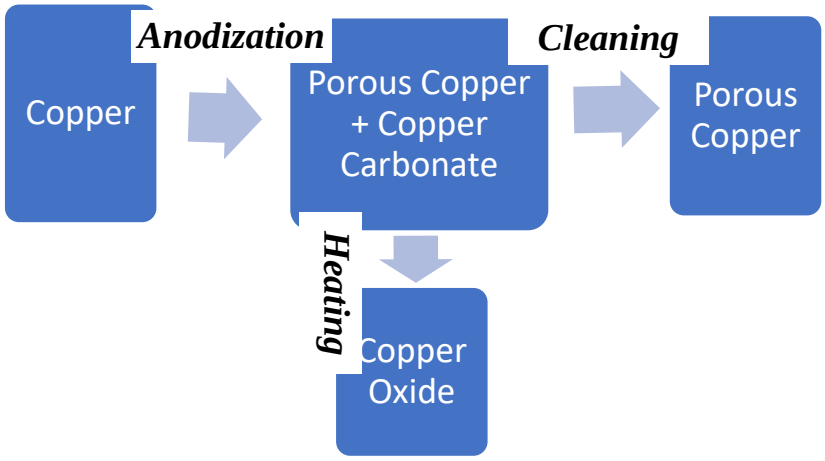

Figure 3.9: Schematic diagram of formation of porous copper and copper oxide

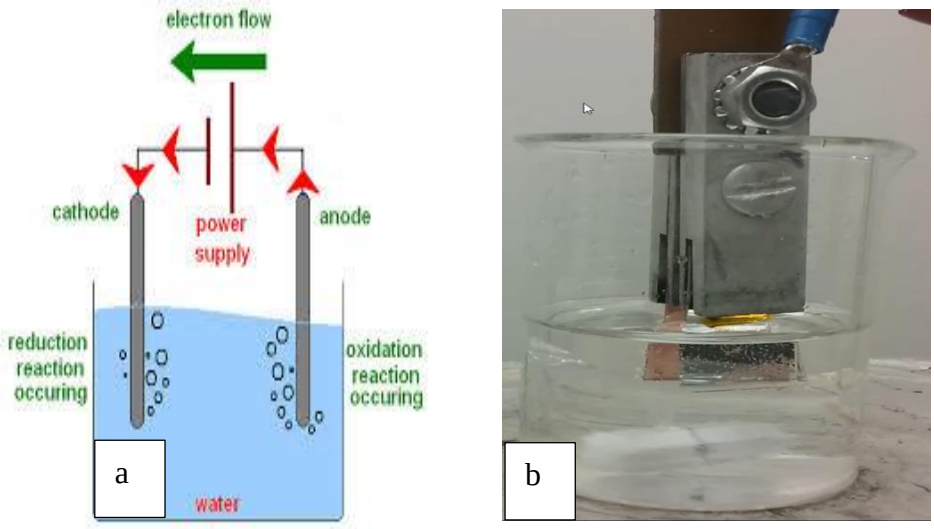

Figure 3.10: Anodic Oxidation Copper Sample(a) Schematic diagram (b) Laboratory Setup

3.2.2 Physical Characterization

The morphology, chemical composition and microstructure of the samples were characterized using a scanning electron microscopy (SEM) on a HITACHI-S3400 as shown in Figure 3.12. SEM images were taken with an accelerating voltage 25kV, working distance on average of 13.4 mm and three different magnifications with 550, 1.10K and 5.50K were employed. The SEM uses a focused beam of high-energy electrons to generate

Figure 3.11: Anodized Copper sample before and after cleaning

Figure 3.12: SEM-EDS Measurement system [66].

a variety of signals at the surface of solid specimens. The signals that derive from electron-sample interactions reveal information about the sample including external morphology (texture), chemical composition, making up the sample[109]. Figure 3.11 above shows the anodized copper sample before and after the cleaning.

The structural composition of the samples was studied by using X-ray diffraction (XRD, D/MAX-RB, Rigaku, Japan) as shown in Figure 3.13 with Cu Kα (1.50598 0A) radiation at 40 kV and 200 mA. The used X-ray diffractometer is the Smart lab and it is one of the high-resolution equipment's available today. The system incorporates a high resolution θ/θ closed loop goniometer drive system, cross beam optics (CBO), an in-plane scattering arm, and an optional 9.0 kW rotating anode generator. Smart Lab Guidance software provides the user with an intelligent interface that guides you through the intricacies of each experiment.

Figure 3.13 X-ray Diffraction Measurement System.

Filmetrics as shown in Figure 3.14 has been used to measure the reflectance of the porous surface of samples. Films as thin as 1nm and as thick as 13 mm can be measured by measuring light not visible to the human eye. Results such as film thickness, color, refractive index, and even roughness are available in seconds. For porous copper, the most fundamental parameters of interest are layer thickness and porosity[109].

Figure 3.14 Reflectance Measurement System [66].

Adhesion test of the copper foil before and after the anodic oxidation was performed by contact angle measurements. The water contact angle measurement of the copper sample was performed by the Data Physics OCA 20 system as shown in Figure 3.15 before and after the oxidation.

Figure 3.15 Contact Angle Measurement system.

3.2.3 Others laboratory setup

These are shown in the Figure 3.16. (a) Ultrasonicator (b) Hotplate, (c) Disc Cutter, (d) Sample, and (e) Vacuum Oven respectively.

Figure 3.16. (a) Ultrasonicator (b) Hotplate, (c) Disc Cutter, (d) Sample, and (e) Vacuum Oven

3.2.4 Slurry Preparation

The working electrode was prepared by a slurry coating method with 80 wt % of active material (AM), 10 wt % of conductive agent (CA), and 10 wt % of binder. NMP was added after stirring the mixture of AM CA for 4 hours by using the magnetic stirrer. The

solvent mixture was stirred for 1h. PVDF as a binder was added with NMP separately and stirred for 1 h and mixed with the solvent mixture of AM and CA. Again, the final mixture was stirred for 4 h. The speed of the magnetic stirrer was 400 rpm and it took 10 hours altogether to get final slurry[110]. Lithium titanate, Li4Ti5O12 was used as a AM and super P carbon black as a CA. Next, the slurry was poured on to the copper foil and ultra-sonicated for 10 minutes before heating. The sample was being kept in vacuum pump at 100 0C for 12 h. Doctor blade was used to maintain the thickness, for this experiment we used 50 μm.

3.2.5 Copper Oxide Synthesis

It was prepared by heating the copper carbonate (Green layer on top of copper) at 200^{o}C for 10 minutes. Copper carbonate on porous copper surface was obtained by anodization of copper. Figure 3.17 shows the Heating of Copper Carbonate.

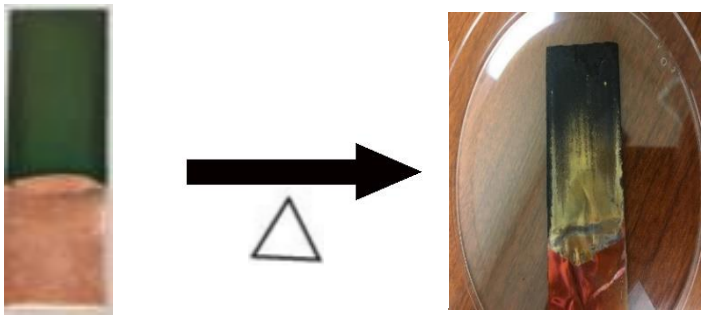

Figure 3.17 Heating of Copper Carbonate

3.2.6 Battery Assembly

Battery fabrication was done inside a Ar-filled glove box. Gloveboxes provide a clean, low-humidity, oxygen free environment for laboratory, cleanroom, electronic

assembly and other critical processing operations in industries such as semiconductor and pharmaceutical manufacturing. The following step was used to assemble the coin cell:

1. Figure 3.18 shows the schematic arrangement of the coin cell assembly.
2. Punch the separator membranes into discs of 15 mm in diameter.
3. Transfer the coin cell cases, springs and spacers, separators and working electrodes into the glove box (after flushing the exchanger three times with argon).
4. Assemble the coin cells in the glove box.
5. Add few drops of the electrolyte on to the cell cup and place the working electrode on it. Add another three drops of the electrolyte and place separator and add two more drops of the electrolyte before placing the lithium counter electrode on it. Place two stainless steel spacers and a spring on the lithium disc.
6. Close the cell using the cell cap and crimp 3-4 times using the compact crimping machine.
7. After assembling the cells, handle the finished cells using plastic tweezers (to avoid short-circuiting).
8. Clean the excess electrolyte leaking from the sides of the cell using a paper napkin.
9. The cell is ready for testing and can be taken out of the glovebox.
10. The fabricated battery was left for at least 12 h for electrolyte wetting stability.

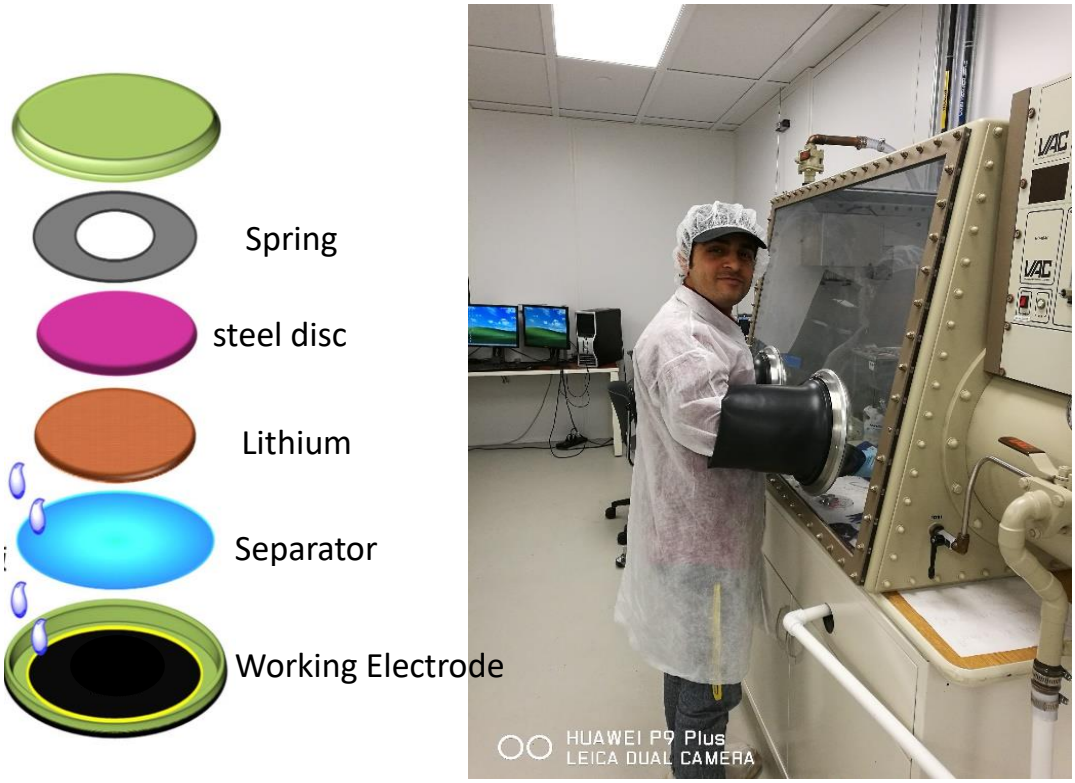

Figure 3.18 Battery Arrangement and Fabrication at Glove Box

3.2.7 Electrochemical Measurements

The electrochemical characterization of the assembled CR2032-type coin cells was done using the LAND CT2001A battery analyzer as shown in Figure 3.19. The cells were galvanostatically charged and discharged at different rates (1C = 170 $mAhg^{-1}$) based on the weight of the anode material in a potential window of 0.01-3V versus Li^{+}/Li at different constant current rate of 0.1C, 0.2C, 0.5C, 1.0C, 2.0C, 5.0C.

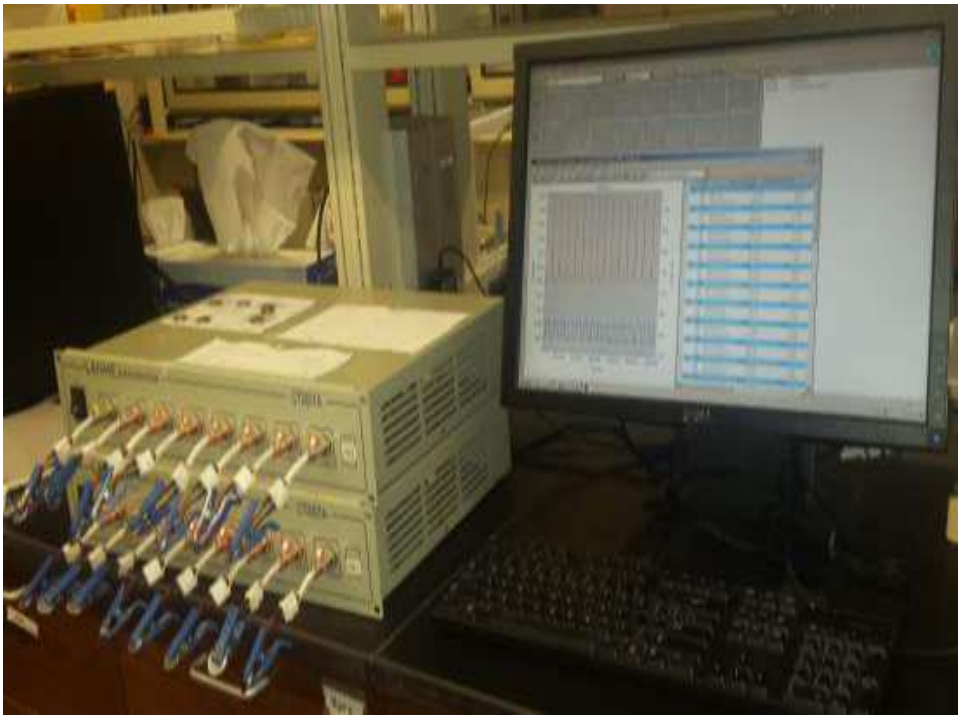

Figure 3.19: LAND CT2001A battery Analyzer system setup.

Cyclic voltammetry (CV) was conducted on an electrochemical workstation of Princeton Applied Research (AMETEK Versa STAT 3) at a scan rate of 0.2 mVs^{-1} from 0.01 to 3.0 V. Electrochemical impedance spectroscopy (EIS) was also performed under the same instrument as shown in figure 3.20. The frequency range from 100 kHz to 0.01 Hz was chosen at the open-circuit potential.

Figure 3.20: System setup used for Electrochemical Impedance (EIS) and Cyclic Voltammetry (CV) measurement

Chapter 4: RESULTS AND DISCUSSIONS

4.1 Morphological Characterization

4.1.1 Anodized Copper

Change in copper surface was observed after the oxidation. The surface of the copper looked darker in color compared to the pristine copper as shown in Figure 4.1showing the anodized copper in the red circles. First the work has been done to optimize the electrolyte composition, ratio of DI water, Glycerol, and Sodium bicarbonate and second task was to optimize the anodization parameter such as applied current, voltage and time. After all the uniform pore on the copper surface has been observed. In figure 4.1 copper surface inside the red region were obtained after the anodization. Surface change can also visualize by naked eye. The copper surface changed to slight dark after the anodization.

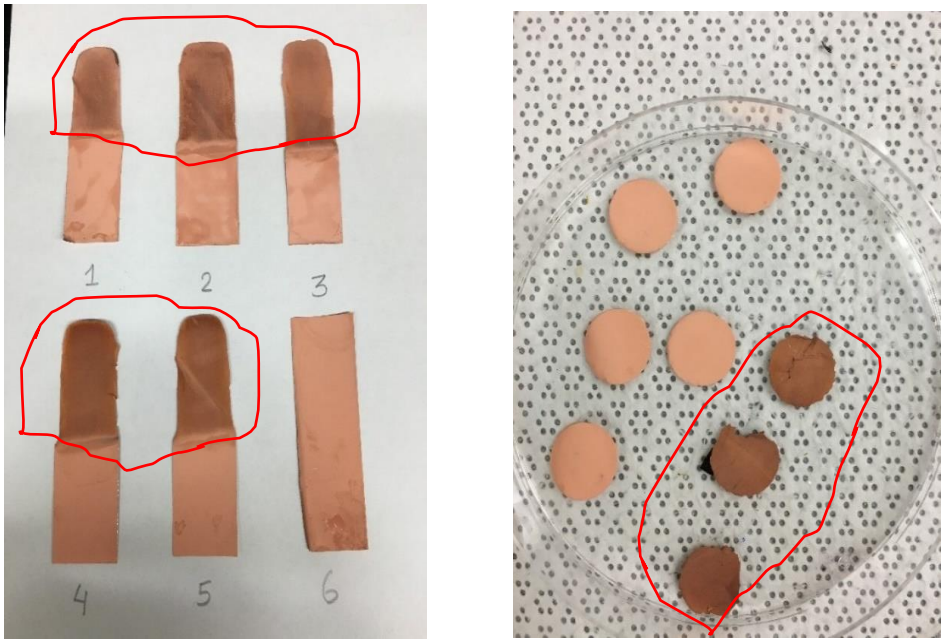

Figure 4.1: Copper surface changed by anodization

Figure 4.2 shows scanning electron microscope (SEM) images of copper surface anodized at constant current mode with different current values of 0.00A, 0.14 A, 0.2 A and 0.6 A for 10 mins. It was observed that when current was increased, the pore diameter also increased until a saturation current. Non-uniform pores started to appear on copper surface for sample anodized at 0.10A. As the current increased from 0.10A, more pores with larger diameter were observed. As seen in the SEM images, uniform pores with larger diameter were only formed at 0.20A. Beyond this saturation current, initial pores etched away and new pores with smaller dimensions appeared when copper was anodized at 0.6 A. In addition, it has been observed that different saturation current occurred for different oxidation time. In addition, small saturation current (0.20A) was enough for longer oxidation time (10min) and large current (2.10A) was required for shorter oxidation time (2min) to get uniform pores formation throughout the copper surface. It can be observed that the average diameter of the pores was about 7μm, which is large enough to accommodate the anode material. The porous structure of the copper enables higher surface area, light weight and high strength structure.

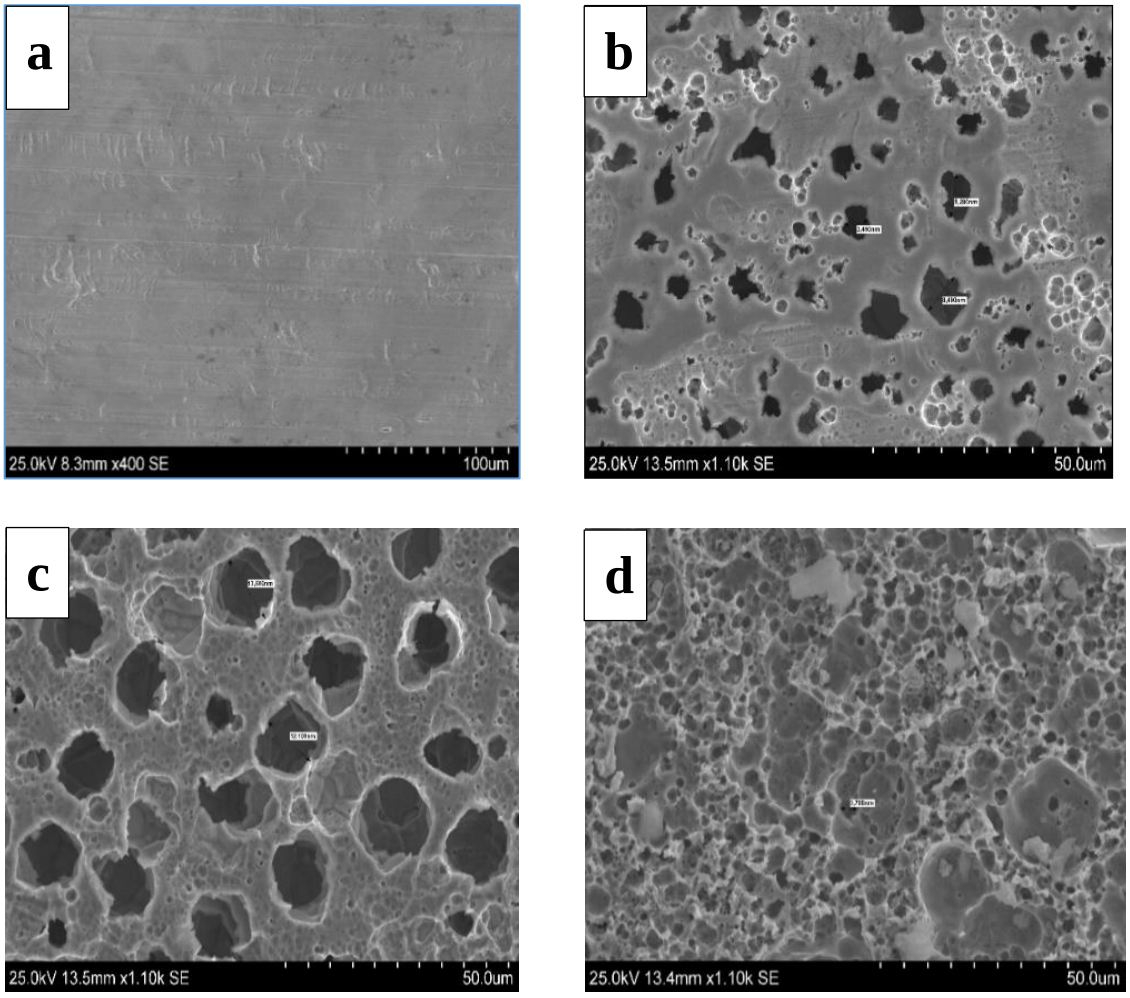

Figure 4.2: SEM images of copper surface anodized at different currents of (a) 0.0A (b) 0.14A (c) 0.2A (d) 0.6A

After optimizing the anodization parameter on copper foil, applied that on the actual current collector foil and the Figure 4.3 was the actual SEM micrographs before and after the oxidation of the current collector foil. SEM images of as received copper foil (A-C) as received and porous copper foil (D-F) with different magnifications at 550, 1.1K and 5.5K respectively. The SEM images show that the anodized copper surface has numerous pores with average pore diameter of 7 μm. The anodization time, applied potential or current density, and concentrations of electrolyte solution determine the number and dimensions of pores [45, 101].

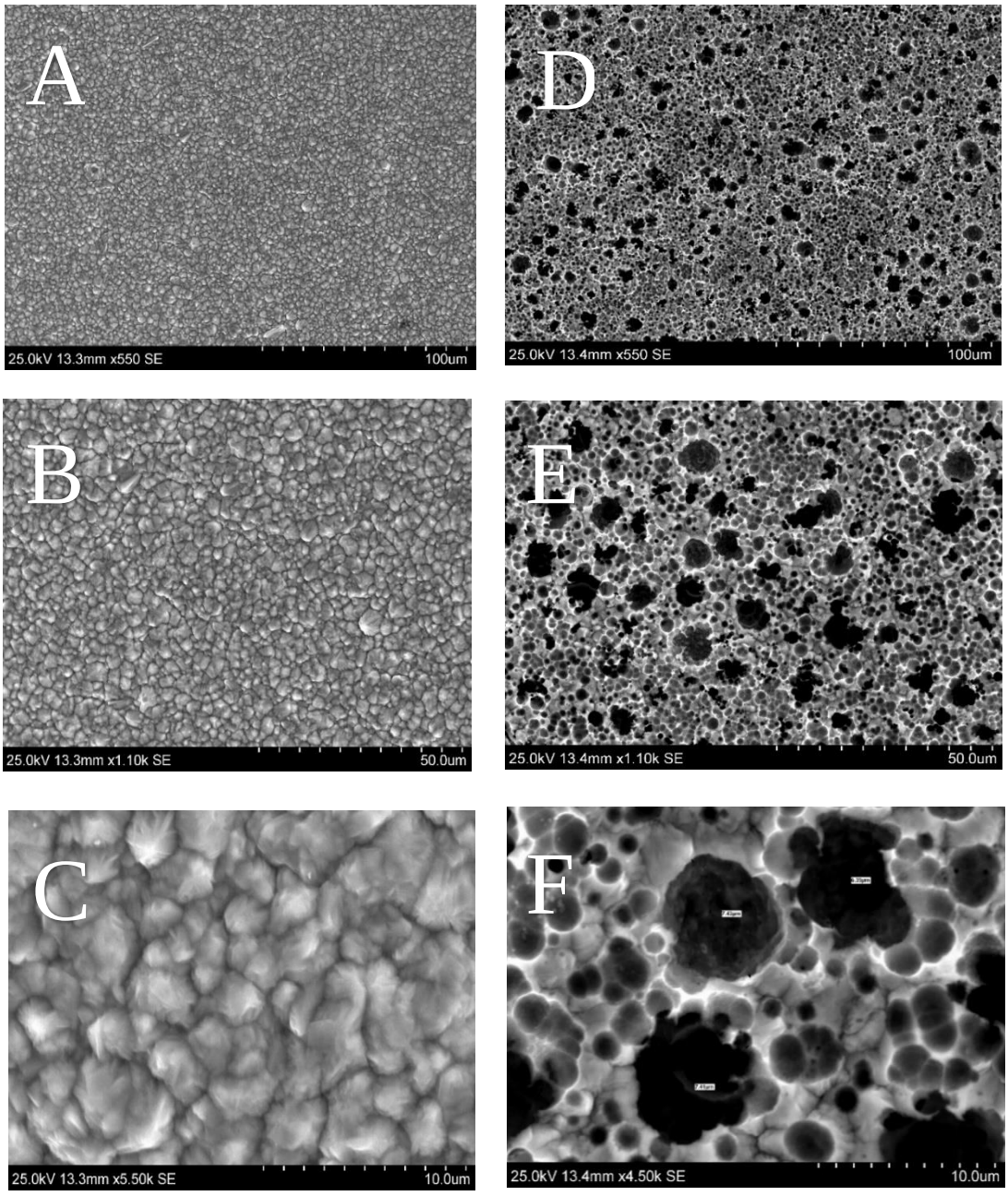

Figure 4.3: SEM micrographs of as received (A-C) and anodized (D-F) copper foil at different magnification

4.1.2 Copper Oxide

Figure 4.4 shows the SEM images of anodized copper foil before (A) and after (B) heating. The anodized copper is covered by a green layer of copper carbonate. Once the carbonate layer was heated at 200°C for 10 mins, it was decomposed into copper oxide and carbon dioxide. As the carbon dioxide evaporated, only copper oxide is remained. The equation can be written as: $\mathrm{CuCO3} \rightarrow \mathit{C}\mathrm{uO} + \mathrm{CO2}$

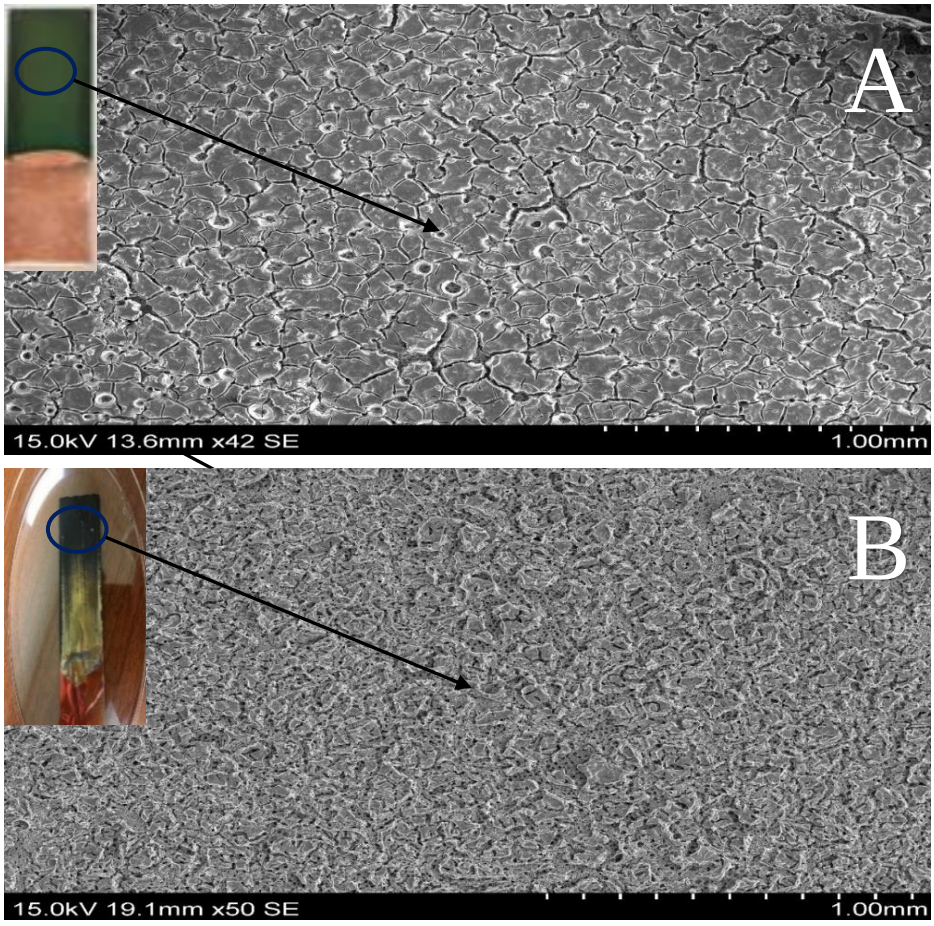

Figure 4.4 SEM images of anodized copper foil before (A) and after (B) heating

4.1.3 Energy-dispersive X-ray spectroscopy (EDX) analysis of copper Oxide

EDX spectroscopy analysis was carried out after the SEM measurement by using the same setup as shown in figure 3.12 above. Figure 4.5 shows the elemental mapping (A) and the distribution of copper (B) and oxygen (C). From the EDX analysis it was obvious that the distribution of copper and oxide throughout the surface was uniform. In addition,

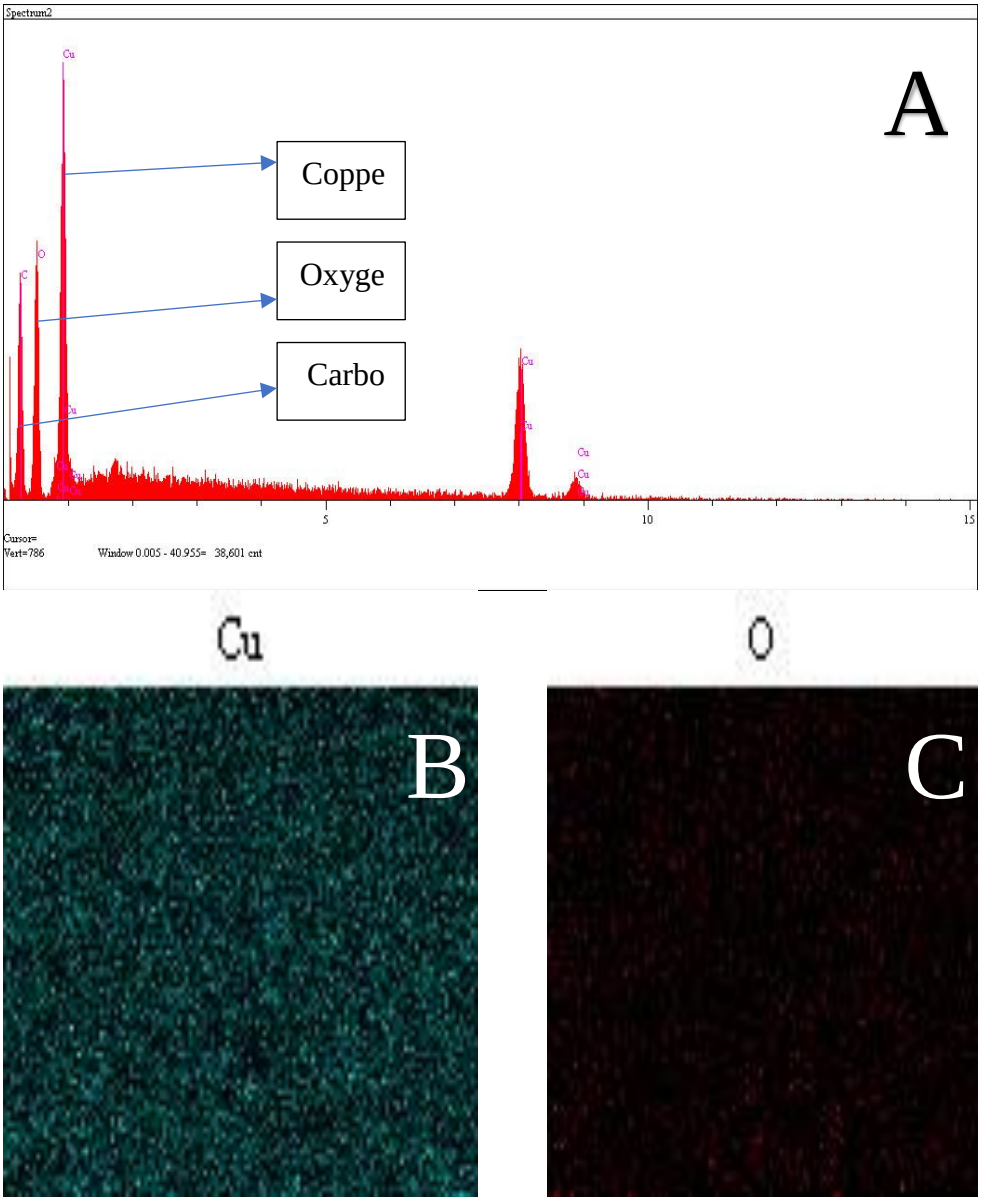

Figure 4.5 Elemental mapping (A) and the distribution of copper (B) and oxygen (C)

the carbon peak along with the copper and oxygen peak shows that the surface also covered with carbon which is in favor with the prompt charge collection for the battery application.

4.1.4 Structural characterization

XRD is used to predict the structural composition on copper before and after oxidation. Figure 4.6 shows the XRD patterns of as-received (non-porous) and oxidized (porous) copper foil. Both the non-porous and porous copper samples had distinct peaks at 43.32^{o}, 50.45^{o}, 74.13^{o}, and 89.94^{o} corresponding to the (111), (200), (220) and (211) planes of Cu respectively. These XRD peaks represented the face-centered cubic copper structure with cell parameter a = b = c = 361.50 pm, $\alpha = \beta = \gamma = 90^{o}$and Z = 4.[111]. It was observed that the peak positions did not change before and after the oxidation, indicating no obvious impurities.

Also, the XRD was used to characterize the formation of copper oxide formed by heating the copper carbonate layer on the copper surface. Figure 4.7 shows the XRD patterns of pure copper and copper oxide. It was found that new peaks at 36.14^{o}, 48.52^{o}, and 60.68^{o} appeared for the copper oxide sample compared to copper sample. Those new peak positions exactly matched with the standard peaks assigned by the PDXL 2 software for copper oxide, indicating the formation of copper oxide after heat treatment.

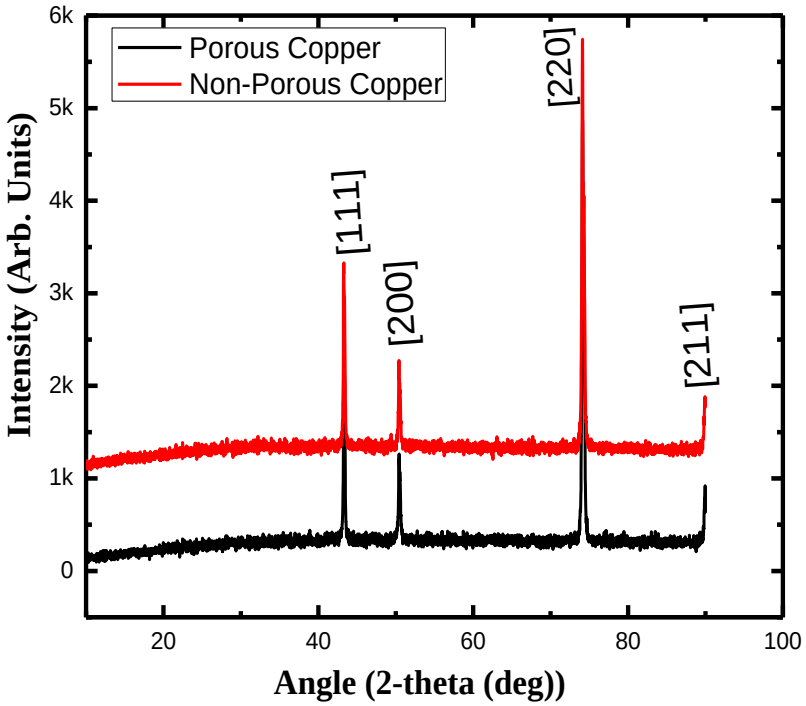

Figure 4.6: XRD pattern of received(Non-Porous) and oxidized(Porous) copper foil

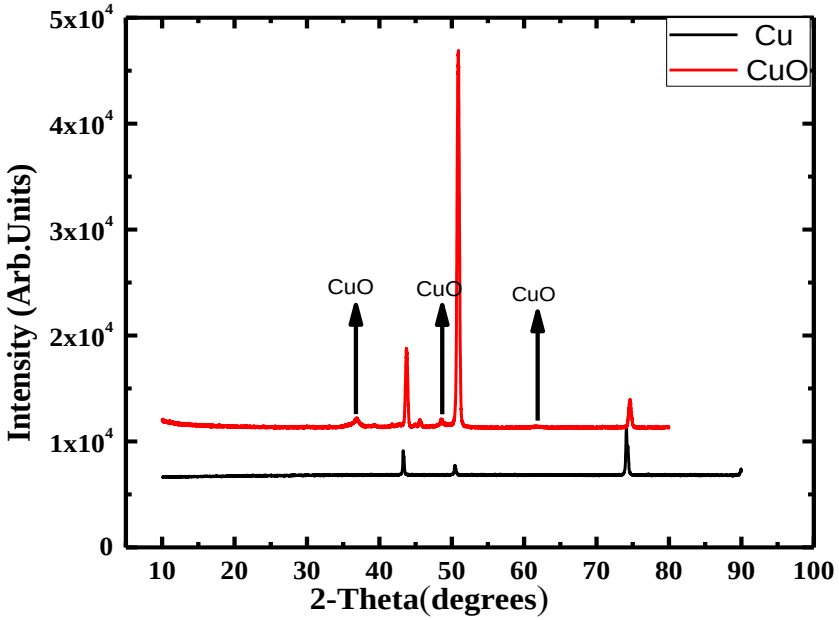

Figure 4.7: XRD pattern of pure copper and copper oxide

4.1.5 Reflectance measurement of porous copper

Reflectance measurement was done using filmetrics f20. The observed reflectance % of all the samples prepared by galvanostatic anodization at the constant current of 0.2A for 10 mins was measured. Figure 4.8 depicts the Reflectance% from received planner (Non-Porous) and anodized (Porous) copper foil. As can be seen, the porous copper foil exhibited reflectance of less than 1%. In comparison, the non-porous copper showed a high reflectance of greater than 40%.

All the samples exhibited reduction in the reflectance in the spectral range of interest from 400 nm to 800 nm. The decrease in the reflectance % can be attributed to the trapping of the light inside the pores. This observation is also a proper indication of formation of the pores throughout the surface of the anodized copper.

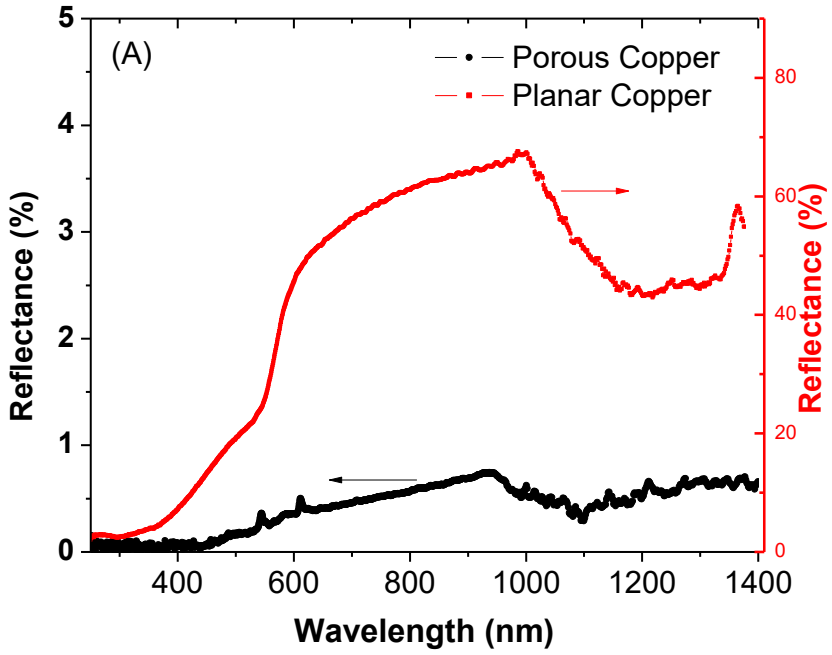

Figure 4.8: Reflectance% from received(Non-Porous) and oxidized(Porous) copper foil

4.2 Adhesion Test

Adhesion tests were done by measuring the contact angle between water and copper surface. Figure 4.9 shows Contact angle measurement between copper, non-porous (A & B) and porous (C & D), and water from left and right. It was observed that the contact angle was reduced from 77.5^{o} to 48^{o} after the oxidation which indicated that the porous surface was more hydrophilic than before. This can allow the electrode slurry to spread easily throughout the surface and help to achieve good adhesion between the current collector and battery electrode. Adhesion between current collector and anode material is very important to achieve stable cycling of a battery especially during high rate charge/discharge processes. At high current charge/discharge, high amount of stress can build up which may lead to electrode peeling off from the copper surface resulting in early battery failure.

Porous copper provides a more hydrophilic surface for battery electrode and can be beneficial for stable battery cycling.

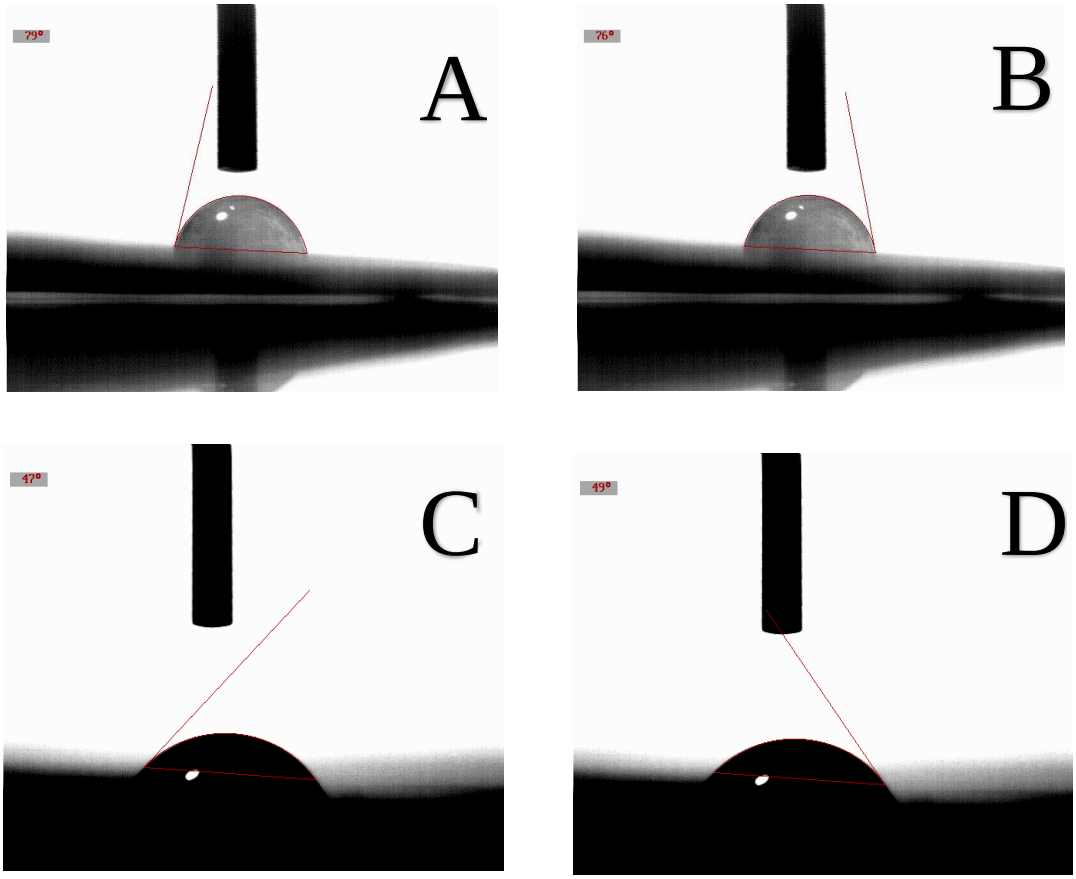

Figure 4.9: Contact angle measurement between copper, non-porous (A & B) and porous (C & D), and water from left and right.

4.3 Absorption measurement of CuO

Figure 4.10 shows the UV-VIS absorbance spectroscopy of copper oxide. The absorbance of the fabricated copper oxide had maximum absorbance in visible region (400-700) nm. The wavelength of the synthesized copper oxide can be calculated as follows:

Band gap (eV) = 1240/ λ (nm) = 1240/1033 = 1.20eV. The CuO can be used for photovoltaic application.

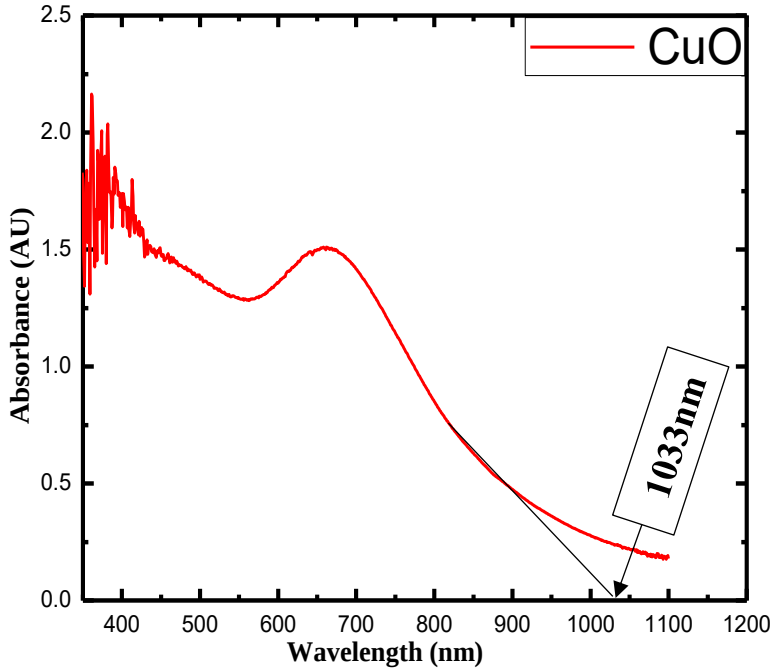

Figure 4.10: UV-VIS absorbance spectroscopy of copper oxide

4.4 Electrochemical charge and discharge cycling performance

Figure 4.11 shows the 2nd cycle charge/discharge voltage profiles of the half cells with lithium titanate as the working electrode on porous and planar copper foils measured at a constant C-rate of 0.1 C. For both the cases of porous and planar copper foils, discharge/charge voltage plateaus were observed about 1.53/1.56 V. However, the reversible discharge capacity for the half cell with porous copper foil was 202.4 mAh/g, which is much higher than that of the planar copper-based cell with 159.2 mAh/g for the second cycle and the corresponding value for the first cycle was 235.8mAh/g and 168.5mAh/g respectively. The higher capacity can be attributed to the enhanced electrochemical lithiation/delithiation or Li^+ transport with the increase in the electrode/electrolyte interface facilitated by the porous structure of the porous copper foil

Figure 4.12 shows the galvanostatic charge/discharge cycling performance of the half cells based on porous and planar copper foils obtained at different C-rates of 0.1C,

0.2C, 0.5C, 1.0C, 2.0C, 5.0C and back to 0.1C. The cell with porous copper exhibited superior rate capability compared to the cell with planar copper foil. The cell with the porous copper retained 95.32% of the initial capacity after cycling at 0.1C, 0.2C, 0.5C, 1.0C, 2.0C and 5.0C rates vs the cell with planar copper with 95.28%. This superior rate capability and stability of the cell with the porous copper current collector can be attributed to the unique properties of the porous copper such as large surface area, highly conductive pathways, short electron and lithium ion diffusion lengths and buffer spaces to accommodate the stress during the cycling processes [15-21].

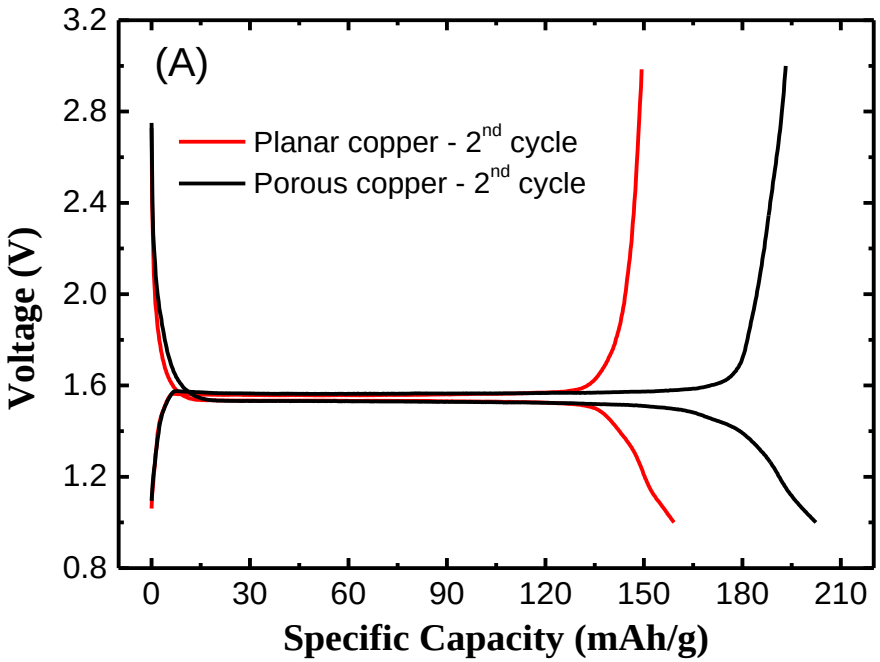

Figure 4.11: Galvanostatic charge-discharge voltage profile for 2nd cycle

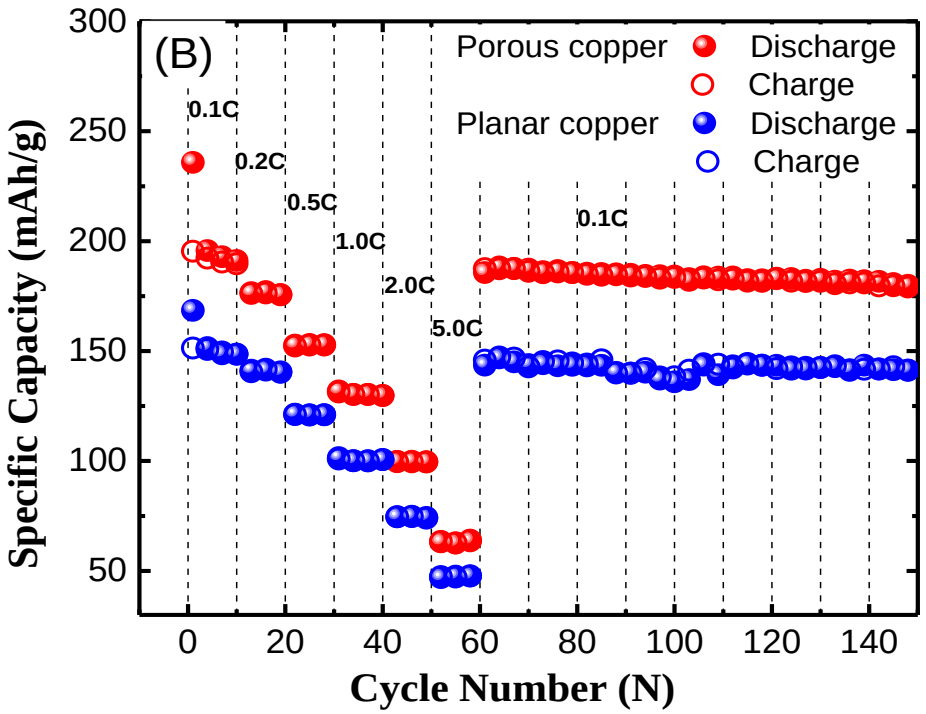

Figure 4.12: Specific capacity vs. cycle number of half-cells on non-porous and porous copper collector at different C-rates

Figure 4.13 shows the specific capacity vs. cycle number of the half-cell CuO as an anode material. The cycle performance shows that the specific capacity at 8th cycle was more than 800 mAhg^{-1} which is higher than reported before. The cycle performance shows that the fabricated copper oxide by novel technique gave high performance[112, 113]. The enhance performance of copper oxide also arouse from the hidden porous structure of the

current collector as well. However, detail properties and reaction mechanism of the copper oxide as an anode material will be the future study of this research work.

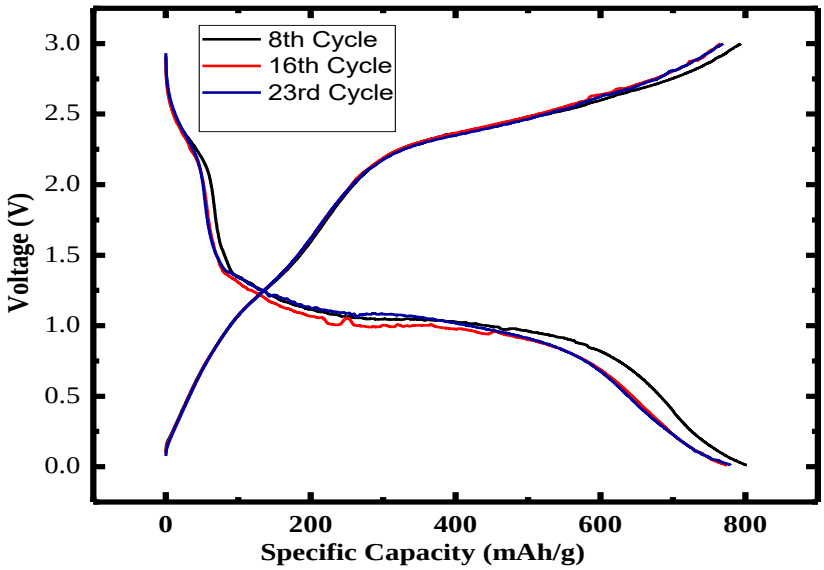

Figure 4.13: Specific capacity vs. cycle number of the half-cell CuO as an anode material

4.5 Cyclic Voltammetry (CV) and Electrochemical Impedance Spectroscopy (EIS)

To understand the difference in the charge/discharge processes for different current collectors, cyclic voltammetry and EIS measurements were performed. Figure 4.14 shows cyclic voltammogram curves of the half-cells with the porous and planar copper as current collector cycled for 150 cycles. Both the cells demonstrated one cathodic peak located at 1.45 V (vs Li) corresponding to Li intercalation into $Li_4Ti_5O_{12}$ and one anodic peak at 1.72 V (vs Li) corresponding to Li deintercalation from $Li_4Ti_5O_{12}$. The cell with the porous copper demonstrated sharper oxidation and reduction peaks with higher values of current density in comparison to the cell with the planar copper. This revealed that the rate of redox

reaction was faster for cell with the porous copper current collector than that of the planar copper current collector. The observation of this electrochemical behavior supports the

$$-Li_7Ti_5O_{12} \rightarrow Li_4Ti_5O_{12} + 3Li^+ + xe^-$$

capacity enhancement observed for the porous copper based cell. As can be seen in the EIS spectra also known as Nyquist plots, shown in Figure 4.15, the charge transfer resistance (represented by diameter of the depressed semicircle) for the porous copper current collector was lower than that the planar copper current collector. This confirms the superior electrode redox kinetics in case of the porous copper current collector compared to the planar copper. Additional advantage of porous copper is to reduce the insignificant mass in the current collector as thinner current collector is important to increase the energy density ($Wh/cm^{2.}$) Oxidation of LTO in the half cell charging process happens as Li^+ is being extracted from charged LTO shown in equation below: On the other hand, reduction of LTO in half cell discharging process happens as Li^+ is being inserted into the LTO layers and the chemical reaction is as follows. This higher redox activity for porous Cu supported

$$-Li_4Ti_5O_{12} + 3Li^+ + 3e^- \rightarrow Li_7Ti_5O_{12}$$

the higher cycling rate performance from the charge/discharge tests.

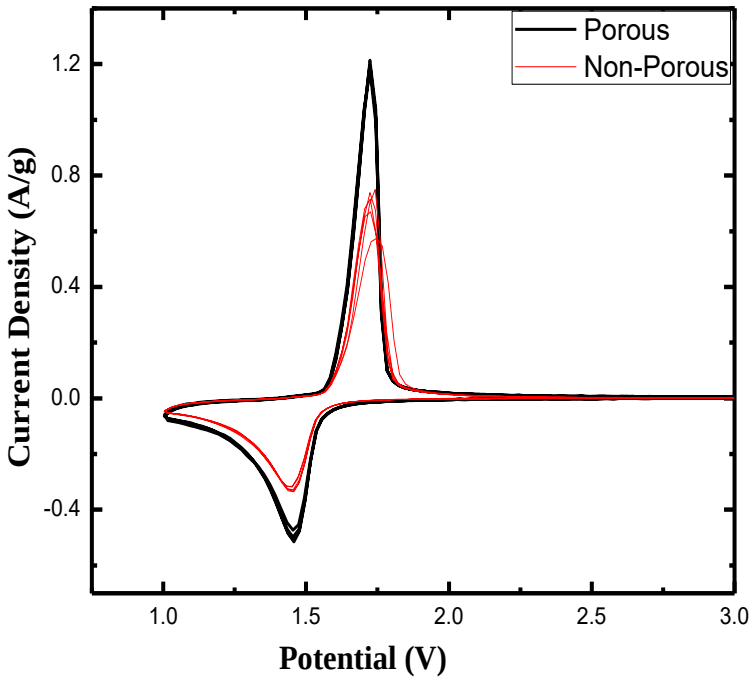

Figure 4.14: Cyclic voltammetry measurement for 5 cycles

45

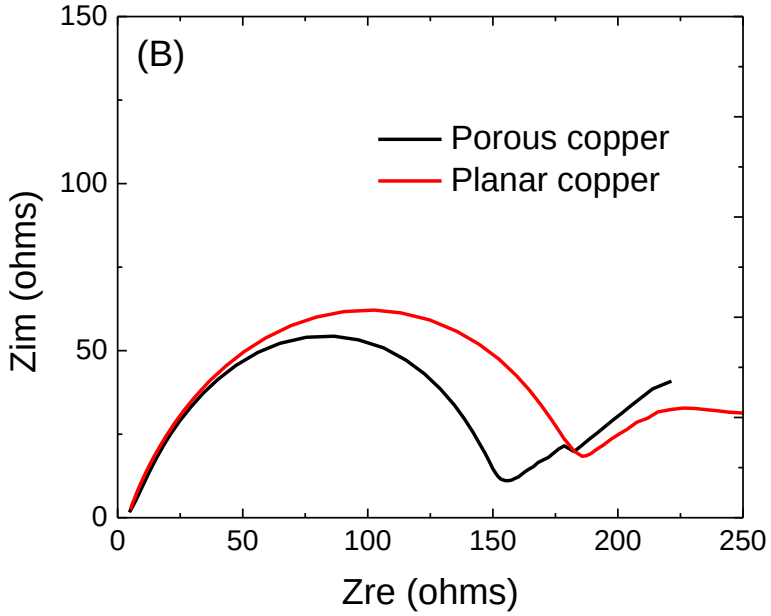

Figure 4.15: EIS measurement of batteries after 150 cycles

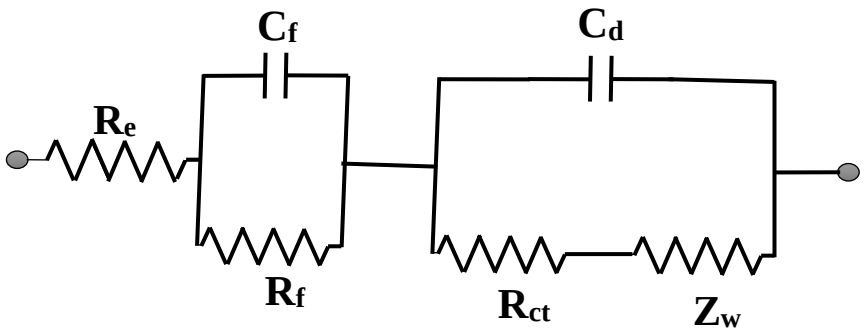

Figure 4.16 Equivalent circuit of half-cell model.

Chapter 5: CONCLUSIONS

5.1 Summary

Many research predicts that the world energy consumption is rapidly increasing day by day and in the future more energy demand is unavoidable fact. Current issue of the 21st century is the energy storage rather than the energy generation. Energy can be generated from the renewable energy sources such as solar, wind etc. To mitigate such demand, several technologies have been developed to enable energy storage such as batteries, supercapacitors, pumped hydro, and flywheel. The above-mentioned energy storage technologies offer the benefit of temporary electricity storage and using it during peak demand hours. In this regard, Secondary batteries seem promising device because of its rechargeable nature although these sounds expensive for the first. Despite the advantage and disadvantage of all the battery prototypes, zinc-carbon and alkaline batteries from the primary battery and nickel cadmium, lead acid and lithium ion from the secondary batteries dominated the market due to their higher specific energy, specific capacity, columbic

efficiency, capacity retention, cycle durability, very low self-discharge rate and more simple charge/discharge cycling properties[114]. Different electrical devices require different energy storage solution. For instance, electric vehicles for consumer use require high capacity batteries to lengthen the travel range between recharging stops. On the other hand, electric buses with regular stops equipped with charging outlets require faster charging electrical energy storage for frequent charging at its designated stops during service hours. Lithium-ion batteries are becoming mainstream battery choice for consumer and automotive applications. As always there is certain challenges often associated with it and the projection of only modest future cost reduction is the biggest challenge and believe it or not, a revolution in lithium ion batteries is in its final stages now. So, small improvement in battery performance and reduction of cost counts[115].

Fabrication of an efficient current collector and binder free copper oxide on top of porous copper, by using a novel, convenient, scalable, efficient, cheapest and environmental friendly way to enhance performance of energy storage device like the specific capacity of LIB at different charging/discharging current rate. The major objective of this research work was to enhance the performance of the lithium-ion battery by using porous copper current collector and binder free copper oxide as battery anode to accomplish the mentioned objectives, the following tasks were performed:

1 Optimize the anodization parameters for copper oxidation.

2 Fabricate and optimize pores on copper foil substrate by anodization.

3 Fabricate the copper oxide by heating after anodization.

4 Fabricate Li-ion half-cells using porous and planner current collector with lithium titanite electrode and investigate charge/discharge performance.

5 Fabricate Li-ion half-cells using electrodeposited copper oxide as potential anode and investigate charge/discharge performance.

Battery is an electrochemical device that converts chemical energy to electrical energy. A battery consists of a multiple number of electro chemical cells. Major attributes of a battery include its capacity, durability, charging time, safety, toxicity and cost which determine the battery market. There are two kinds of battery available: non-rechargeable (Primary) and rechargeable (Secondary) batteries. Primary Batteries are designed to be used until the energy is exhausted and need to be replaced with a new one. There chemical reactions are not reversible but can be used immediately after the fabrication. However, secondary batteries can be recharged since their chemical reactions are reversible but are required to be charged before use[91]. In lithium ion battery, metal oxide works as cathode and carbon-based material typically graphite works as an anode and electrolyte is a lithium salt dissolved in an organic solvent. The two electrodes are separated by a polymer separator membrane for electrical isolation but the membrane is ionically conducting[49]. Discharge of a battery happens by oxidation of anode or reduction of cathode and reverse happens during charging. Variety of materials can be employed as electrodes in lithium ion batteries and different performance level can be achieved.

Porous copper has been fabricated by various method and most popular methods are Casting, Powder Metallurgy, Dealloying and Electrodeposition and also there are

different technique to synthesis copper oxide. However, the abovementioned methods are demanding and not environmental friendly and which limits its use in industrial application. But there is a need for a cost-effective and non-toxic anodization technique to obtain highly ordered porous copper for the use as an efficient current collector and copper oxide as a binder free anode material for Lithium battery application. The major goal of this research was to develop a cost effective and non-toxic technique to fabricate porous copper and copper oxide for energy storage application. Porous copper and copper oxide can be use in various devices as per their demand. For instance, sensor, supercapacitor, solar cell, battery and in most cases wherever copper has been using that can be replace by porous copper for more efficient and sensitive device[45,116-122].

Formation of porous copper involves two simultaneous process one after another, oxidation followed by dissolution of copper. The most important factor for pore formation is availability of valance band hole which is primarily determined by the dopants, electrolyte concentration, back illumination and applied electric field. Similarly, copper oxide fabrication also happens in two steps. First, deposition of carbonate layer on surface of porous copper and heating of copper carbonate. The reason behind to use the glycerol based electrolyte for electrochemical anodization was to get the uniform porous structure throughout the surface and carbonate layer can go inside of every pore. Once the copper carbonate is heated copper oxide can be formed inside of each pore which improve adhesion force. Electrolyte was the composition of glycerol, DI water and Sodium bicarbonate. The separation between cathode and anode were 1 cm apart and applied a galvanostatic mode. Uniform pores were observed at 0.2 A for 10-minute anodization time. However, for different current different time can make same pore. During the experiment, it has been observed that higher current need less time and vice versa.

5.2 Conclusions

This novel technique to fabricate porous copper and copper oxide on porous copper has several advantages such as low cost, non-toxic, environmental friendly and less corrosive electrochemical technique can be used to fabrication and the beauty of this experiment was both porous copper and copper oxide can fabricate by using the same technique and same setup. The only difference in the experiment is if porous copper is needed then wash the anodized sample by IPA and if copper oxide is needed heated the sample for 10 minutes at 200^{o} C. One of its great emerging advantage is its commercialized nature as a current collector (porous copper) and anode material (copper oxide) for lithium ion battery. The objective of porous efficient current collector and advanced anode material was achieved using constant current anodization technique. Same pore morphology and copper carbonate layer can be achieved at different parameter. However, green layer of copper carbonate will be deposited more easily on the copper surface for longer time or higher current. Fabricated battery using porous current collector has more specific capacity and less impedance. Similarly, battery using the copper oxide on porous copper current collector gives batter performance. Porous copper and copper oxide both can be commercialized in lithium ion battery and so on.

5.3 Future Work

Future work should include investigation of the effect of porous copper current collector for material having high specific capacity like silicon for Li-ion batteries and the fabrication of the sensor and supercapacitor using porous copper and copper oxide. The most importantly it seems useful for the integrated device having battery and solar cell on each side.

REFERENCES

1. Naderi, R., *Composite Gel Polymer Electrolyte for Lithium Ion Batteries.* 2016.
2. Pérez-Lombard, L., J. Ortiz, and C. Pout, *A review on buildings energy consumption information.* Energy and buildings, 2008. **40**(3): p. 394-398.
3. Randers, J., *" A global Forecast for the next 40 years" Available:* http://www.2052.info/. 2015.
4. Cotterman, T., *Energy storage technologies: transforming America's intelligent electrical infrastructure.* 2013.
5. Tarascon, J.M. and M. Armand, *Issues and challenges facing rechargeable lithium batteries.* Nature, 2001. **414**(6861): p. 359-367.
6. Blomgren, G.E., *The Development and Future of Lithium Ion Batteries.* Journal of The Electrochemical Society, 2017. **164**(1): p. A5019-A5025.
7. *"History of the battery".* Wikipedia (The Free Encyclopedia) Available : https://en.wikipedia.org/wiki/History_of_the_battery, 2015.
8. "History of Battery" Battery University, Available: http://batteryuniversity.com/learn/article/when_was_the_battery_invented, 2017.
9. BUG, G., *"Early Innovators".* Battery University, Available: http://batteryuniversity.com/learn/article/battery_developments, 2017.
10. *" The History of Battery" Wikipedia, the free encyclopedia, Available:* https://en.wikipedia.org/wiki/History_of_the_battery. 2016.
11. Levi, O., *Alessandro Volta and the Voltaic Pile.* Available: https://orenteach.files.wordpress.com/2011/01/oren-volta-final-project.pdf, 2011.
12. Jenson, W.B., *"The Edison Nickel-Iron Alkaline Storage Cell," Available:* https://drc.libraries.uc.edu/bitstream/handle/2374.UC/702761/The-Daniell-Cell.pdf?sequence=1. Museum Notes, October 2013.
13. Gurung, A., et al., *Tin Selenide–Multi-Walled Carbon Nanotubes Hybrid Anodes for High Performance Lithium-Ion Batteries.* Electrochimica Acta, 2016. **211**: p. 720-725.
14. Kim, J.Y. and D.Y. Lim, *Surface-modified membrane as a separator for lithium-ion polymer battery.* Energies, 2010. **3**(4): p. 866-885.
15. Brinker, C., *Hydrolysis and condensation of silicates: effects on structure.* Journal of Non-Crystalline Solids, 1988. **100**(1-3): p. 31-50.
16. DeMar, P.J. *Nickel-Iron*. in *Telecommunications Energy Conference (INTELEC), 2011 IEEE 33rd International*. 2011. IEEE.
17. Park, K.-H., et al., *Effects of HNO 3 treatment of TiO 2 nanoparticles on the photovoltaic properties of dye-sensitized solar cells.* Materials Letters, 2009. **63**(26): p. 2208-2211.
18. Novák, P., et al., *Electrochemically active polymers for rechargeable batteries.* Chemical Reviews, 1997. **97**(1): p. 207-282.

19. Yata, S., *Electrically conductive organic polymeric material and process for production thereof*. 1986, Google Patents.
20. Yata, S., K. Tanaka, and T. Yamabe. *Polyacene (PAS) Bátteries*. in *MRS Proceedings*. 1997. Cambridge Univ Press.
21. Goodenough, J.B. and Y. Kim, *Challenges for rechargeable Li batteries.* Chemistry of Materials, 2009. **22**(3): p. 587-603.
22. Rolison, D.R., *Zeolite-modified electrodes and electrode-modified zeolites.* Chemical Reviews, 1990. **90**(5): p. 867-878.
23. Rolison, D.R., et al., *Multifunctional 3D nanoarchitectures for energy storage and conversion.* Chemical Society Reviews, 2009. **38**(1): p. 226-252.
24. Banhart, J., *Manufacture, characterisation and application of cellular metals and metal foams.* Progress in Materials Science, 2001. **46**(6): p. 559-632.
25. Kreuzeder, M., et al., *Fabrication and thermo-mechanical behavior of ultra-fine porous copper.* Journal of materials science, 2015. **50**(2): p. 634-643.
26. Niu, J., et al., *Effect of Electrodeposition Parameters on the Morphology of Three-Dimensional Porous Copper Foams.* Int. J. Electrochem. Sci, 2015. **10**: p. 7331-7340.
27. Ru, J., et al., *Porous copper with capillary performance and gas permeability prepared by two-step foaming method.* International Journal of Precision Engineering and Manufacturing, 2015. **16**(7): p. 1461-1466.
28. Waters, C., M. Salih, and S. Ajinola, *Porosity comparative analysis of porous copper and OOF modelling.* Journal of Porous Materials, 2015. **22**(4): p. 989-995.
29. Park, J., et al., *Effect of transference velocity and hydrogen pressure on porosity and pore morphology of lotus-type porous copper fabricated by a continuous casting technique.* Acta Materialia, 2007. **55**(16): p. 5646-5654.
30. Wang, N., et al., *Role of surfactants in construction of porous copper film by electrodeposition approach.* Transactions of the IMF, 2011. **89**(5): p. 261-267.
31. Bianchi, E., et al., *Heat transfer properties of metal foam supports for structured catalysts: wall heat transfer coefficient.* Catalysis today, 2013. **216**: p. 121-134.
32. Choi, Y.-S., H.-R. Yu, and H.-W. Cheong, *Electrochemical properties of a lithium-impregnated metal foam anode for thermal batteries.* Journal of Power Sources, 2015. **276**: p. 102-104.
33. Tsai, B.-T., et al., *Effects of flow field design on the performance of a PEM fuel cell with metal foam as the flow distributor.* international journal of hydrogen energy, 2012. **37**(17): p. 13060-13066.
34. Tseng, C.-J., et al., *A PEM fuel cell with metal foam as flow distributor.* Energy Conversion and Management, 2012. **62**: p. 14-21.
35. Ahmed, Y., et al., *Correlation between factors controlling preparation of porous copper via sintering technique using experimental design.* Powder technology, 2007. **175**(1): p. 48-54.
36. Ide, T., A. Tsunemi, and H. Nakajima, *Fabrication of porous copper with directional pores by continuous casting technique through thermal decomposition of hydride.* Metallurgical and Materials Transactions B, 2014. **45**(4): p. 1418-1424.

37. Luo, B., et al., *3D Porous Copper Films with Large Specific Surface Prepared by Hydrogen Bubble Template.* Asian Journal of Chemistry, 2013. **25**(17): p. 9927.
38. Najdovski, I. and A.P. O'Mullane, *The effect of electrode material on the electrochemical formation of porous copper surfaces using hydrogen bubble templating.* Journal of Electroanalytical Chemistry, 2014. **722**: p. 95-101.
39. Nakajima, H. and T. Ide, *Fabrication of porous copper with directional pores through thermal decomposition of compounds.* Metallurgical and Materials Transactions A, 2008. **39**(2): p. 390-394.
40. Nikolić, N.D. and G. Branković, *Comparison of open porous copper structures obtained by the different current regimes of electrolysis.* Materials Letters, 2012. **70**: p. 11-15.
41. Shapovalov, V. and L. Boyko, *Gasar—a new class of porous materials.* Advanced engineering materials, 2004. **6**(6): p. 407-410.
42. Nikolić, N.D., G. Branković, and K.I. Popov, *Optimization of electrolytic process of formation of open and porous copper electrodes by the pulsating current (PC) regime.* Materials Chemistry and Physics, 2011. **125**(3): p. 587-594.
43. Ru, J., et al., *Microstructure and sound absorption of porous copper prepared by resin curing and foaming method.* Materials Letters, 2015. **139**: p. 318-321.
44. Zhang, Y., et al., *Hierarchical architectures of monodisperse porous Cu microspheres: synthesis, growth mechanism, high-efficiency and recyclable catalytic performance.* Journal of Materials Chemistry A, 2014. **2**(30): p. 11966-11973.
45. Li, Y., et al., *Superhydrophobicity of 3D porous copper films prepared using the hydrogen bubble dynamic template.* Chemistry of Materials, 2007. **19**(23): p. 5758-5764.
46. Liu, P. and K. Liang, *Review Functional materials of porous metals made by P/M, electroplating and some other techniques.* Journal of Materials Science, 2001. **36**(21): p. 5059-5072.
47. Shin, H.-C. and M. Liu, *Copper foam structures with highly porous nanostructured walls.* Chemistry of materials, 2004. **16**(25): p. 5460-5464.
48. Liu, L., et al., *Preparations and Properties of Porous Copper Materials for Lithium-Ion Battery Applications.* Chemical Engineering Communications, 2016. **203**(6): p. 707-713.
49. Jiang, T., et al., *A three-dimensional cellular copper prepared by multiple-step electrodeposition.* Electrochemical and Solid-State Letters, 2008. **11**(5): p. D50-D52.
50. Xue, L.-J., et al., *Lithium storage performance and interfacial processes of three dimensional porous Sn–Co alloy electrodes for lithium-ion batteries.* Electrochimica Acta, 2011. **56**(17): p. 5979-5987.
51. Jiang, T., et al., *Preparation and characterization of silicon-based three-dimensional cellular anode for lithium ion battery.* Electrochemistry communications, 2007. **9**(5): p. 930-934.

52. Xu, W., et al., *An approach to make macroporous metal sheets as current collectors for lithium-ion batteries.* Journal of The Electrochemical Society, 2010. **157**(7): p. A765-A769.
53. Huang, L., et al., *Electrodeposition and lithium storage performance of three-dimensional porous reticular Sn–Ni alloy electrodes.* Electrochimica Acta, 2009. **54**(10): p. 2693-2698.
54. Huang, L., et al., *Electrodeposition and lithium storage performance of novel three-dimensional porous Fe–Sb–P amorphous alloy electrode.* Electrochemistry Communications, 2009. **11**(3): p. 585-588.
55. Jiang, T., et al., *Preparation and characterization of tin-based three-dimensional cellular anode for lithium ion battery.* Journal of Power Sources, 2007. **166**(2): p. 503-508.
56. Huang, X., et al., *Nickel foam-supported porous NiO⁄Ag film electrode for lithium-Ion batteries.* Journal of the Electrochemical Society, 2008. **155**(6): p. A438-A441.
57. Shin, H.C. and M. Liu, *Three-Dimensional Porous Copper–Tin Alloy Electrodes for Rechargeable Lithium Batteries.* Advanced Functional Materials, 2005. **15**(4): p. 582-586.
58. Hassoun, J., et al., *High-Rate, Long-Life Ni–Sn Nanostructured Electrodes for Lithium-Ion Batteries.* Advanced Materials, 2007. **19**(12): p. 1632-1635.
59. Ke, F.-S., et al., *Three-dimensional nanoarchitecture of Sn–Sb–Co alloy as an anode of lithium-ion batteries with excellent lithium storage performance.* Journal of Materials Chemistry, 2012. **22**(34): p. 17511-17517.
60. Taberna, P.-L., et al., *High rate capabilities Fe3O4-based Cu nano-architectured electrodes for lithium-ion battery applications.* Nature materials, 2006. **5**: p. 567-573.
61. El-Hadek, M.A. and S. Kaytbay, *Mechanical and physical characterization of copper foam.* International Journal of Mechanics and Materials in Design, 2008. **4**(1): p. 63-69.
62. Grootenhuis, P., R. Powell, and R. Tye, *Thermal and electrical conductivity of porous metals made by powder metallurgy methods.* Proceedings of the Physical Society. Section B, 1952. **65**(7): p. 502.
63. Yang, G.F., K.Y. Song, and S.K. Joo, *A metal foam as a current collector for high power and high capacity lithium iron phosphate batteries.* Journal of Materials Chemistry A, 2014. **2**(46): p. 19648-19652.
64. Etiemble, A., et al., *3D morphological analysis of copper foams as current collectors for Li-ion batteries by means of X-ray tomography.* Materials Science and Engineering: B, 2014. **187**: p. 1-8.
65. Needham, S.A., et al., *Electrochemical performance of Co3O4–C composite anode materials.* Electrochemical and solid-state letters, 2006. **9**(7): p. A315-A319.
66. Poizot, P., et al., *Nano-sized transition-metal oxides as negative-electrode materials for lithium-ion batteries.* Nature, 2000. **407**(6803): p. 496-499.

67. Zheng, S.-F., et al., *Introducing dual functional CNT networks into CuO nanomicrospheres toward superior electrode materials for lithium-ion batteries.* Chemistry of Materials, 2008. **20**(11): p. 3617-3622.
68. Grugeon, S., et al., *Combining electrochemistry and metallurgy for new electrode designs in Li-ion batteries.* Chemistry of materials, 2005. **17**(20): p. 5041-5047.
69. Mitra, S., et al., *Growth and electrochemical characterization versus lithium of Fe3O4 electrodes made by electrodeposition.* Advanced Functional Materials, 2006. **16**(17): p. 2281-2287.
70. Taberna, P.-L., et al., *High rate capabilities Fe3O4-based Cu nano-architectured electrodes for lithium-ion battery applications.* Nature materials, 2006. **5**(7): p. 567-573.
71. Gillot, F., et al., *Electrochemical reactivity and design of NiP2 negative electrodes for secondary Li-ion batteries.* Chemistry of materials, 2005. **17**(25): p. 6327-6337.
72. Zhou, Z., et al., *Binder Free Hierarchical Mesoporous Carbon Foam for High Performance Lithium Ion Battery.* Scientific Reports, 2017. **7**.
73. Li, Y., B. Tan, and Y. Wu, *Ammonia-evaporation-induced synthetic method for metal (Cu, Zn, Cd, Ni) hydroxide/oxide nanostructures.* Chemistry of Materials, 2007. **20**(2): p. 567-576.
74. Lu, Y., et al., *Macroporous Co 3 O 4 platelets with excellent rate capability as anodes for lithium ion batteries.* Electrochemistry Communications, 2010. **12**(1): p. 101-105.
75. Yuan, L., et al., *Spherical clusters of NiO nanoshafts for lithium-ion battery anodes.* Electrochemical and solid-state letters, 2006. **9**(11): p. A524-A528.
76. Li, X., et al., *Binder-free porous core–shell structured Ni/NiO configuration for application of high performance lithium ion batteries.* Electrochemistry Communications, 2010. **12**(9): p. 1222-1225.
77. Aricò, A.S., et al., *Nanostructured materials for advanced energy conversion and storage devices.* Nature materials, 2005. **4**(5): p. 366-377.
78. Li, H., et al., *Research on Advanced Materials for Li-ion Batteries.* Advanced Materials, 2009. **21**(45): p. 4593-4607.
79. Reddy, M., G. Subba Rao, and B. Chowdari, *Metal oxides and oxysalts as anode materials for Li ion batteries.* Chemical reviews, 2013. **113**(7): p. 5364-5457.
80. Xu, X., et al., *Nanostructured transition metal sulfides for lithium ion batteries: Progress and challenges.* Nano Today, 2014. **9**(5): p. 604-630.
81. Chen, X., N. Zhang, and K. Sun, *Facile fabrication of CuO mesoporous nanosheet cluster array electrodes with super lithium-storage properties.* Journal of Materials Chemistry, 2012. **22**(27): p. 13637-13642.
82. Gao, S., et al., *Green fabrication of hierarchical CuO hollow micro/nanostructures and enhanced performance as electrode materials for lithium-ion batteries.* The Journal of Physical Chemistry C, 2008. **112**(49): p. 19324-19328.
83. Pan, Q. and J. Liu, *Facile fabrication of porous NiO films for lithium-ion batteries with high reversibility and rate capability.* Journal of Solid State Electrochemistry, 2009. **13**(10): p. 1591-1597.

84. Wang, H., et al., *Improving electrochemical performance of NiO films by electrodeposition on foam nickel substrates.* Journal of applied electrochemistry, 2009. **39**(9): p. 1597-1602.
85. Gao, X., et al., *Preparation and electrochemical performance of polycrystalline and single crystalline CuO nanorods as anode materials for Li ion battery.* The Journal of Physical Chemistry B, 2004. **108**(18): p. 5547-5551.
86. Sahay, R., et al., *High aspect ratio electrospun CuO nanofibers as anode material for lithium-ion batteries with superior cycleability.* The Journal of Physical Chemistry C, 2012. **116**(34): p. 18087-18092.
87. Shi, L., et al., *Synthesis of different CuO nanostructures from Cu (OH) 2 nanorods through changing drying medium for lithium-ion battery anodes.* RSC Advances, 2015. **5**(36): p. 28611-28618.
88. Wang, C., et al., *Morphology-dependent performance of CuO anodes via facile and controllable synthesis for lithium-ion batteries.* ACS applied materials & interfaces, 2014. **6**(2): p. 1243-1250.
89. Zhu, Y., et al., *Facile fabrication of three-dimensional hierarchical CuO nanostructures with enhanced lithium storage capability.* RSC Advances, 2015. **5**(83): p. 68061-68066.
90. Li, J., et al., *Thermally oxidation synthesis of CuO nanoneedles on Cu foam and its enhanced lithium storage performance.* Journal of Materials Science: Materials in Electronics, 2017. **28**(3): p. 2353-2357.
91. Fulcomer, P.M., *Prospects for the Use of Lithium Batteries in Law Enforcement Equipment*. 1990: US Department of Justice, Office of Justice Programs, National Institute of Justice.
92. ITCA, *"A Guide to Lead-Acid Batteries" Available:* http://www.itacanet.org/a-guide-to-lead-acid-battries/part-1-how-lead-acid-batteries-work/. 2017.
93. Shukla, A., S. Venugopalan, and B. Hariprakash, *Nickel-based rechargeable batteries.* Journal of Power Sources, 2001. **100**(1): p. 125-148.
94. Gurung, A., et al., *Highly Efficient Perovskite Solar Cell Photocharging of Lithium Ion Battery Using DC–DC Booster.* Advanced Energy Materials, 2017.
95. Varapragasam, S.J., et al., *Kirkendall Growth of Hollow Mn3O4 Nanoparticles upon Galvanic Reaction of MnO with Cu2+ and Evaluation as Anode for Lithium-Ion Batteries.* The Journal of Physical Chemistry C, 2017. **121**(21): p. 11089-11099.
96. Matthey, J., *How cells work, Available:* http://www.jmbatterysystems.com/technology/cells/how-cells-work. 2014.
97. *MIT Electric Vehicle Team "A Guide to Understanding Battery Specifications" Available:* http://web.mit.edu/evt/summary_battery_specifications.pdf. 2008.
98. Dunn, B., H. Kamath, and J.-M. Tarascon, *Electrical energy storage for the grid: a battery of choices.* Science, 2011. **334**(6058): p. 928-935.
99. Hyun, S., K. Murakami, and H. Nakajima, *Anisotropic mechanical properties of porous copper fabricated by unidirectional solidification.* Materials Science and Engineering: A, 2001. **299**(1): p. 241-248.

100. Hyun, S. and H. Nakajima, *Anisotropic compressive properties of porous copper produced by unidirectional solidification.* Materials Science and Engineering: A, 2003. **340**(1): p. 258-264.
101. Hyun, S. and H. Nakajima, *Effect of solidification velocity on pore morphology of lotus-type porous copper fabricated by unidirectional solidification.* Materials Letters, 2003. **57**(21): p. 3149-3154.
102. Zhao, Y., et al., *Lost carbonate sintering process for manufacturing metal foams.* Scripta Materialia, 2005. **52**(4): p. 295-298.
103. Aburada, T., J.M. Fitz-Gerald, and J.R. Scully, *Synthesis of nanoporous copper by dealloying of Al-Cu-Mg amorphous alloys in acidic solution: The effect of nickel.* Corrosion Science, 2011. **53**(5): p. 1627-1632.
104. Dan, Z., et al., *Fabrication of nanoporous copper by dealloying of amorphous Ti–Cu–Ag alloys.* Journal of Alloys and Compounds, 2014. **586**: p. S134-S138.
105. Hayes, J., et al., *Monolithic nanoporous copper by dealloying Mn–Cu.* Journal of Materials Research, 2006. **21**(10): p. 2611-2616.
106. Liu, D., et al., *Preparation of 3D nanoporous copper-supported cuprous oxide for high-performance lithium ion battery anodes.* Nanoscale, 2013. **5**(5): p. 1917-1921.
107. Lu, H.-B., Y. Li, and F.-H. Wang, *Synthesis of porous copper from nanocrystalline two-phase Cu–Zr film by dealloying.* Scripta materialia, 2007. **56**(2): p. 165-168.
108. Shoesmith, D., et al., *Anodic oxidation of copper in alkaline solutions: Part IV. Nature of the passivating film.* Journal of Electroanalytical Chemistry and Interfacial Electrochemistry, 1983. **143**(1-2): p. 153-165.
109. Microscopy, S.E., *"Surface Morphology" Available:* http://serc.carleton.edu/research_education/geochemsheets/techniques/SEM.html. 2017.
110. Kraytsberg, A. and Y. Ein-Eli, *Conveying Advanced Li-ion Battery Materials into Practice The Impact of Electrode Slurry Preparation Skills.* Advanced Energy Materials, 2016.
111. Krishnamoorthy, K. and S.-J. Kim, *Growth, characterization and electrochemical properties of hierarchical CuO nanostructures for supercapacitor applications.* Materials Research Bulletin, 2013. **48**(9): p. 3136-3139.
112. Li, J., et al., *Thermally oxidation synthesis of CuO nanoneedles on Cu foam and its enhanced lithium storage performance.* Journal of Materials Science: Materials in Electronics: p. 1-5.
113. Tan, G., et al., *Freestanding three-dimensional core-shell nanoarrays for lithium-ion battery anodes.* Nature communications, 2016. **7**.
114. Peng, X., et al., *A high-performance electrospun thermoplastic polyurethane/poly (vinylidene fluoride-co-hexafluoropropylene) gel polymer electrolyte for Li-ion batteries.* Journal of Solid State Electrochemistry, 2016. **20**(1): p. 255-262.
115. Lee, D., *"Improving Lithium Ion Battery for Future Energy Storage Needs" Available:* http://www.batterypoweronline.com/main/articles/improving-lithium-ion-battery-for-future-energy-storage-needs/. 2016.

116. Crick, C.R., J.A. Gibbins, and I.P. Parkin, *Superhydrophobic polymer-coated copper-mesh; membranes for highly efficient oil–water separation.* Journal of Materials Chemistry A, 2013. **1**(19): p. 5943-5948.
117. Levitsky, I., et al., *Hybrid solar cells based on porous Si and copper phthalocyanine derivatives.* Applied physics letters, 2004. **85**(25): p. 6245-6247.
118. Suk, J., et al., *Electrodeposited 3D porous silicon/copper films with excellent stability and high rate performance for lithium-ion batteries.* Journal of Materials Chemistry A, 2014. **2**(8): p. 2478-2481.
119. Yu, L., et al., *3D porous gear-like copper oxide and their high electrochemical performance as supercapacitors.* CrystEngComm, 2013. **15**(38): p. 7657-7662.
120. Cheng, H., et al., *Organic dyes containing indolodithienopyrrole unit for dye-sensitized solar cells.* Dyes and Pigments, 2018. **149**: p. 16-24.
121. Su, J., et al., *New triarylamine organic dyes containing the 9-hexyl-2-(hexyloxy)-9H-carbazole for dye-sensitized solar cells.* Electrochimica Acta, 2017. **254**: p. 191-200.
122. Wu, Y., et al., *Influence of Nonfused Cores on the Photovoltaic Performance of Linear Triphenylamine-Based Hole-Transporting Materials for Perovskite Solar Cells.* ACS Applied Materials & Interfaces, 2018. **10**(21): p. 17883-17895.